TECHNICAL MEMORANDUMS

NATIONAL ADVISORY COMMITTEE FOR AERONAUTICS

No. 941

SOME DATA ON THE STATIC LONGITUDINAL STABILITY AND CONTROL OF AIRPLANES (DESIGN OF CONTROL SURFACES)

By A. Martinov and E. Kolosov

Central Aero-Hydrodynamical Institute

Washington
May 1940

NATIONAL ADVISORY COMMITTEE FOR AERONAUTICS

TECHNICAL MEMORANDUM NO. 941

SOME DATA ON THE STATIC LONGITUDINAL STABILITY AND CONTROL OF AIRPLANES*

(DESIGN OF CONTROL SURFACES)

By A. Martinov and E. Kolosov

1. STATEMENT OF THE PROBLEM

In connection with the increasing demands made on the maneuverability and controllability of modern airplanes, the question of the so-called "allowable degree of stability" has lost that clarity with which a number of authors have sought to define it (reference 1). There has arisen the necessity of building airplanes with a smaller reserve of stability, thereby approaching the "neutral" type. The problem of controllability and maneuverability can not otherwise be satisfactorily solved with the modern methods of airplane control.

In line with this tendency toward airplanes with a small reserve of stability considerably stricter conditions are imposed on the airplane design and increased demands are made on the pilot. At the same time, greater responsibility is laid on the computer since small errors in computation may lead to an unstable airplane.

Fundamental in the computation of the static stability is the determination of the correct center of gravity position, shape of wing and method of attachment so as to assure small moments of the entire airplane without tail. The choice of the tail itself is generally determined by the following methods:

1) Method of selecting the tail surfaces from wind-tunnel tests.

2) Method based on the comparison of curves obtained from tests on models of the airplane elements.

3) Analytical method.

*Report No. 278, of the Central Aero-Hydrodynamical Institute, Moscow, 1936.

In our opinion the first method is impracticable since it not only requires a large amount of wind-tunnel work but is at the same time a "blind" method. The second method is most widely applied by aircraft designers. The third method has come to attract more and more attention. Comparisons made of computations, wind-tunnel tests and flight tests indicate the very great possibilities of the method, particularly for preliminary approximations. The problem is logically expressed in the form of seeking the limiting center-of-gravity positions for which the airplane is still able to satisfy the stability requirements put on it.

There are naturally two such center-of-gravity positions to be considered, namely, the forward and backward positions. For an airplane of the usual arrangement, the first corresponds to the limiting angle of deflection of the control surface and the limiting force on the control stick in landing.

For an accurate determination of these values, it is necessary to establish standards of allowable limiting forces acting on the control stick. It must be said that information in this connection is not available in the engineering literature and these standards must be newly established, based on full-scale tests on airplanes.

The second limiting center-of-gravity position corresponds to the state of the airplane at which it becomes entirely neutral.*

A detailed analysis shows that the limiting forward center-of-gravity position must be determined in landing with deflected flap and account must be taken of the ground

---

*After this paper had been written, there appeared the work of V. S. Pishnov, "Aerodynamics of the Airplane," Part II, in which the author has introduced the conception of critical center of gravity position only for $\frac{\partial C_{mz}}{\partial \alpha} = 0$, i.e., corresponding to the neutral state of the airplane. We considered it useful, however, to introduce the conception of still another limiting center-of-gravity position determined by the maximum possible force on the pilot's stick. These two magnitudes will then satisfactorily solve the problem of center-of-gravity position. Moreover, in designating a limiting backward center-of-gravity position, it is necessary to take account of the dynamic stability of the airplane.

effect on the airplane characteristics. The limiting backward center-of-gravity position in the computation is obtained in "hands-off" flight. These two cases should be investigated in determining the center-of-gravity position of the airplane.

The analytical method of computation in combination with the accumulated mean characteristics of airplane elements at the present time may serve as the most reliable method, since it combines the advantages of correspondence to actual conditions with clearness of a picture of the phenomenon, thus permitting a conscious improvement of the balancing and stability.

It would be quite incorrect to say that the analytical method of computation is rendered entirely feasible by the amount of data available. In regard to some subjects, as for example, the effects of interference between elements of the airplane on the stability, the data are as yet too meager to allow any general conclusions to be drawn. It is clear that in such cases more factual material obtained from wind-tunnel and flight tests is required. The most rational method of computation thus appears to be a combination of the analytical supplemented by curves obtained from tests on models, and, as more data are accumulated, the part played by the supplementary tests will become smaller and smaller.

Notation Adopted

C_m, pitching-moment coefficient

C_{m_w}, moment coefficient of wing

C_{m_f}, moment coefficient of fuselage

$C_{m_{int}}$, moment coefficient arising from wing-fuselage interference

$C_{m_{lg}}$, moment coefficient of landing gear

C_{m_T}, moment coefficient due to propeller thrust

C_{m_t}, moment coefficient of tail

C_y, C_x, C_n, C_t, coefficients of aerodynamic forces

C_h, hinge moment of control surface

S, area

b, chord

l, span

t, mean chord of servo-control tab = S_{sc}/l_{sc}

L, distance from center of gravity of airplane to hinge of control surface

x/b, position along longitudinal axis of center of gravity (sign + is taken in direction toward tail)

y/b, position along vertical axis of center of gravity (sign + for down direction)

$$n = \sqrt{\frac{S_{cont\ surf}}{S_{tail}}}$$

V, speed

α, angle of attack

δ, angle of deflection of control surface (sign + for down deflection)

θ, angle of deflection of servo control (sign + for down deflection)

φ, angle of deflection of stabilizer (+ upward)

$K, = \frac{\theta}{\delta}$ kinematic coefficient of linkage between servo-control and main-control surface

$K_1 = \partial C_h/\partial\alpha$

$K_2 = \partial C_h/\partial\delta$

$m_\alpha = \frac{\partial C_m}{\partial C_y}$ at δ = const (see section 5)

$q_\delta = \frac{\partial C_m}{\partial C_y}$ at α = const (see section 11)

R, Reynolds number

ϵ, measure of the turbulence, $\epsilon = \frac{\sqrt{(\Delta \bar{V})^2}}{V_{mean}}$

Subscripts

a,	airplane	T,	thrust
w,	wing	sc,	servo control
t,	tail	st,	stabilizer
f,	fuselage	int,	interference
lg,	landing gear	cs,	control surface

The basic equation of the equilibrium of the moments acting on the airplane about its center of gravity in its plane of symmetry may be written in the following nondimensional form

$$C_{m_w} + C_{m_f} + C_{m_{int}} + C_{m_{lg}} + C_{m_T} + C_{m_t} = C_{m_a} \qquad (1)$$

Of these coefficients C_{m_w}, $C_{m_{lg}}$, C_{m_T}, and C_{m_t} may be computed. The effect of the fuselage, however, and the interference effect of the airplane elements must be determined from test data.

Differentiating equation (1) with respect to α we obtain the condition for the limiting aft location of the center of gravity.

$$\frac{\partial C_{m_w}}{\partial \alpha} + \frac{\partial C_{m_f}}{\partial \alpha} + \ldots + \frac{\partial C_{m_t}}{\partial \alpha} = 0 \qquad (2)$$

The center of gravity position is found from the component $\frac{\partial C_{m_w}}{\partial \alpha}$, in which it enters.

$$\frac{\partial C_{m_w}}{\partial \alpha} = \frac{\partial C_{m'}}{\partial \alpha} - \frac{x}{b}\frac{\partial C_n}{\partial \alpha} + \frac{y}{b}\frac{\partial C_t}{\partial \alpha} \qquad (3)$$

The effect of the center-of-gravity location on the other moments acting on the airplane is negligible by comparison with the moment of the wing.

The basic moment, which the pilot is capable of changing in flight, is the tail moment C_{m_t}

$$C_{m_t} = C_{y_t}\frac{S_t L_t}{S_t b_w}\left(\frac{V_t}{V}\right)^2 \qquad (4)$$

since with modern airplane arrangements C_n may be replaced by C_y and the moment due to C_t may be neglected even for neutral airplanes for which the accuracy requirements are raised, and C_{y_t} may be expressed in the simplest case of control surface without balance and cut-out

$$C_{y_t} = \frac{\partial C_y}{\partial \alpha_t}\left[\alpha_t + n\delta_{cs}\right] \qquad (5)$$

Let us now consider what change is introduced into the phenomenon by the condition of free control stick. We shall simplify the picture by not touching upon the dynamic elements of the phenomenon. The control surface, which is statically balanced, is adjusted with respect to the flow in such a manner that it forms with the stabilizer a certain angle δ_2 (fig. 1). The airplane trimmed by the pilot to a certain attitude with the aid of the control surface inclined at the angle δ_1 immediately passes into the other attitude corresponding to the deflection δ_2 the value of which may be found from the condition of zero value of the hinge moment.

$$C_h = \frac{\partial C_h}{\partial \alpha_t}\alpha_t + \frac{\partial C_h}{\partial \delta_{cs}}\delta_2 = K_1\alpha_t + K_2\delta_2 = 0 \qquad (6)$$

A linear dependence of this kind may, as shown by tests, be applied to the fundamental types of tail surfaces within the range below flow separation. Therefore

$$\delta_2 = - \frac{K_1}{K_2} \alpha_t \tag{7}$$

Thus

$$C_{y_t} = \frac{\partial C_y}{\partial \alpha_t} \left[\alpha_t - n \frac{K_1}{K_2} \alpha_t \right] = \frac{\partial C_y}{\partial \alpha_t} \alpha_t \left(1 - n \frac{K_1}{K_2} \right) \tag{8}$$

By formulas (7) and (8) it is possible to estimate the changes both of C_{y_t} and the derivatives: $\frac{\partial C_m}{\partial \alpha}$; $\frac{\partial C_y}{\partial \alpha}$; $\frac{\partial C_m}{\partial C_y}$; for choice of center-of-gravity location and solution of the problem of stability with controls free.

The weight of the control surface may be taken into account without any difficulty. In place of equation (6), we must write

$$M_h - M_{wt} = 0 \tag{9}$$

or, denoting the weight of the control surface by G_{cs}, the lever arm with respect to the hinge axis by r_{cs} and the inclination of the wing chord of the airplane to the horizontal by ϵ

$$\rho S_{cs} V_x^2 b_{cs} (K_1 \alpha_t + K_2 \delta_2) - G_{cs} r_{cs} \cos(\delta_2 + \epsilon + \varphi_{st} - \Delta\alpha) = 0$$

Taking

$$\cos(\delta_2 + \epsilon + \varphi_{st} - \Delta\alpha) = 1$$

we obtain

$$\delta_2 = \frac{G_{cs} r_{cs}}{K_2 \rho S_{cs} V_x^2 b_{cs}} - \frac{K_1}{K_2} \alpha_t \tag{10}$$

$$C_{y_t} = \frac{\partial C_y}{\partial \alpha_t}\left[\alpha_t\left(1 - n\frac{K_1}{K_2}\right) + \frac{n\, G_{cs}\, r_{cs}}{K_2\, \rho\, S_{cs}\, V_t^{\,2}\, b_{cs}}\right] \quad (11)$$

The influence of the weight on the effectiveness of the tail surfaces with controls free is taken into account by the last term of equation (11).

In the case of present day airplanes with considerably increasing speeds, the controls are balanced as regards their weight to prevent vibration of the tail so that the last term of equation (11) becomes zero.

In flying the airplane with stick free, an additional loss in stability is encountered as a result of the decrease in effectiveness of tail surfaces provided with a servo-balance tab connecting with the stick. We shall return to this question in considering servo-balance and servo-control tabs.

It is thus clear that a preliminary computation of the longitudinal center-of-gravity location that basically solves the problem of longitudinal static stability may be made, provided certain magnitudes are known among which

$$n, \quad K_1, \quad K_2, \quad \frac{\partial C_y}{\partial \alpha_t}, \quad \frac{\partial C_y}{\partial \delta}$$

are the most important. At the present time a sufficiently large amount of experimental material has been accumulated, enabling all the above-enumerated magnitudes to be computed with an accuracy sufficient for a first computation. It will be our object to give data for the preliminary computation of these magnitudes. This procedure is followed, notwithstanding the existence in some of the cases considered of formulas since these formulas, on the one hand, are less accurate and, on the other, include a somewhat narrower range of tail-surface designs.

In this work, moreover, we attempted to throw light on the action of the servo control, servo balance and trimming tabs. These investigations were included in view of the unusual interest in this question and the wide application of these devices in modern airplane design.

Since the concept of "axial balance" appears to be generally known, no explanations will be given in this regard. As far as servo control is concerned, however, we consider it necessary to present a certain brief discussion.

At the present time the term "servo controls" is understood to mean surfaces located aft of the control members for the object of decreasing the control forces. The principle upon which the action of these surfaces is based is the setting up of an additional moment balancing the hinge moment of the main-control surface when the angle at which the servo-control surface is set with respect to the mean surface is varied. Servo controls therefore, in contrast to other types of balance devices are controllable devices.* According to the character of the control, servo controls are divided into servo controls properly so-called and "servo balancers."

If the change in the setting of the servo control with respect to the main-control surface (free in the given case) is effected by the pilot by means of a device connecting only with the servo control we have a servo control proper, i.e., we have the following scheme of action of the servo control. The pilot deflects the servo-control surface from its initial position by a certain angle and under the action of the moment set up the entire system consisting of the main free control surface and the controllable servo surface is set in motion and settles at a position of equilibrium when the resulting moment about the axis of rotation of all the applied forces on the entire control system becomes equal to zero. A sketch of this system of servo control is given in figure 2.

If the change in the angle of setting of the servo control is effected by the pilot through the intermediary action of the main-control surface then we have the "servo balance flaps" or tab. In this case, the servo control is connected with the main control by a mechanism which, on rotating the main-control surface, rotates the servo-control surface in the opposite direction as a result of which the balancing moment is set up. A sketch of this control arrangement is shown on figure 3. The rod a connects the servo surface to the stabilizer by means of the bars b and c which lie on straight lines passing through the axes of

*An exception is formed only in the case of the adjustable type servo controls where the trailing edges of the control members are capable of being deflected on the ground.

rotation of the main- and servo-control surfaces and perpendicular to the common chord. When b and c, the distances from the axes of rotation to the hinges of the rod a, are equal, angles θ and δ will be equal for the entire range of deflection of the main-control surface and hence the chord of the servo control will at all times be parallel to the stabilizer chord. Denoting the ratio $\frac{\theta}{\delta}$ by K, then for $b = c$, $K = 1$. As may be readily seen on figure 3, if $b > c$, $K < 1$ and conversely, if $b < c$, $K > 1$. Hence, by increasing or decreasing the value of b keeping c constant, we shall obtain different values for K and therefore different degrees of balance for a given servo-control tab.

Finally, the servo control may be replaced by movable stabilizer which we shall call a tab. The latter and the main-control surface have controls independent of each other. In changing the setting of the tab with respect to the main control, there is obtained the same effect as in changing the setting of the stabilizer. The deflection of the tab by a certain angle makes possible zero pressure on the control stick for any state of flight of the airplane.

In recent times, servo-balance tabs and trimming tabs have received very wide application to airplanes of all sizes and purposes and are mounted on all control members - vertical and horizontal tail surfaces and ailerons. Servo controls proper, on the other hand, are rarely used in their original form and are met with exclusively on heavy airplanes.

Besides appearing to be one of the best means of balnacing as compared with other types (axial, horn, servo control) servo-balance flaps possessthe property that they permit easy regulation of the degree of balance to any required limit by means of a simple change in the ratio $K = \frac{\theta}{\delta}$, a change which may be easily effected after the first trial flight.

A control system provided with a servo-control tab is a mechanical system with a great number of degrees of freedom as compared with the system provided with the servo-balance tab and therefore appears less reliable with regard to vibration. Moreover, a system with servo balance does not

deprive the pilot of his sense of controlling the airplane as is the case with the servo control proper. All these clear advantages of the servo balance give it first place as compared with servo control.

In the present paper we shall consider the action of servo controls mainly as servo-balance tabs so that in what follows, unless otherwise stated, wherever we speak of servo controls we shall refer to servo-balance flaps or tabs.

The theory of the action of servo controls has been given by Glauert (reference 2) for the case of thin profiles with hinged flap in two-dimensional, parallel flow. This theory may be applied to the case of the control surface with servo control alone, i.e., without stabilizer. A further development of this theory of Glauert has been given by Perring (reference 3) for the case of a wing with an entire system of hinged flaps and hence this theory makes it possible to compute the most important case arising in practice, namely, a tail unit consisting of a stabilizer, main-control surface, and servo-control tabs.

In formulating our program it was initially proposed to carry out tests with the object of checking the existing theories on servo controls in order to find correction coefficients for passing from theory to experiment and finally to devise, on the basis of existing theory, a procedure for the computation and selection of servo controls for a given tail surface. From a comparison of the theoretical and experimental data, however, it became apparent that the differences between them in some cases amounted to 100 percent and more, the deviation not remaining constant or in any case such that some mean values for the correction factors could be chosen. The choice of correction factors thus presented no fewer difficulties than would be met with in a direct reduction of the experimental data with the derivation, on the basis of this reduction, of purely empirical formulas. It was therefore decided, in view of the fact that existing theory gives a very large disagreement with experimental results and moreover does not take into account a large number of important factors arising in the action of a tail with servo control, such as axial balance and the properties of the profile section selected, to work out on the basis of the experimental data a procedure for the computation of servo controls and the derivation of the necessary experimental formulas.

2. DESCRIPTION OF THE MODEL TAIL SURFACES TESTED AND THEIR CHARACTERISTICS

Considering the large variations that we see at the present time in the choice of wing sections, the question of the section used for the tail surface does not stand out so sharply, inasmuch as the choice of tail surfaces differs essentially from that of the wing and the range of angles at which the tail surfaces operate is not large. Moreover, the distortion of the section by the deflection of the control surface is so large that the smoothness of the flow at any section is rapidly destroyed as the control surface is deflected and as the section assumes a sharp-edged contour. The tail-surface section is generally chosen symmetrical with sufficiently small profile drag for the undeflected surface. The application of nonsymmetrical sections is obviously not logical, since without increasing the effectiveness such sections result in an increase in the hinge moments and drag. As worked-up data in our laboratories and those of the N.A.C.A. show at a certain angle α, a change in thickness has an effect on the value of $\frac{\partial c_y}{\partial \alpha}$ for the section sometimes amounting to 10 percent. For a given profile series a certain thickness is found most advantageous as regards $\frac{\partial c_y}{\partial \alpha}$. The effect of the camber of a nonsymmetrical profile section is replaced by the change in the angle of setting of the tail surface with symmetrical section.

For tail surfaces, section M-2, M-3, and their modifications are widely applied. For fast airplanes, sections with sharp leading edge are to be recommended.

The aspect ratios of tail surfaces in recent times have shown a tendency to decrease, a fact that is explained by considerations of increase in stiffness and avoidance of vibration. The aspect ratio for modern horizontal tail surfaces is generally taken from 3 to 4.

The plan form of the tail surface is extremely arbitrary since the tail surface is generally an element of the architectural design of the airplane, at times to the detriment of its aerodynamics. In recent times, however, the

predominating forms are rectangular and tapered plan forms rounded out by arcs of circles and giving sufficiently good aerodynamic characteristics. In general, however, the effect of the plan form on the tail characteristics, where there is no deviation from simple shapes, is not large.

In this work we shall present a systematized outline of the results of tests on models of tail surfaces both schematized as well as corresponding to actual airplanes. All the models were of a sufficiently large scale (from 1/3 to 1/5) and were tested in the T-1 wind tunnel of the CAHI in the period 1932-1935. An exception is formed only by model N16, which was tested in the 1.5 m tunnel No. 3.

Tail surfaces Nos. 1, 2, 3, 4, 5, 7, 8, and 9, are schematized models; Nos. 6, 11, 12, 13, 14, 15, 16, 17, 18, and 19, are models of actual tail surfaces of airplanes.

Most of the tail surfaces corresponding to actual airplanes had cut-outs, which were for the purpose of mounting the rudder. In recent times, however, there has been noted a tendency toward decreasing or completely eliminating this type of cut-out. As became clear from the results of tests, this tendency of designers is certainly well grounded since a decrease in the cut-out shows up to advantage on the tail characteristics and particularly on the values C_x and $\frac{\partial C_y}{\partial \delta}$. The amount of cut-out in modern airplanes varies between the following limits: for heavy airplanes, 5 to 7 percent of the elevator area; for average-size airplanes, 10 to 17 percent; and for light airplanes, up to 25 percent of the control surface. In the present paper, we have attempted to estimate the effect of cut-outs on the aerodynamics of the tail surfaces.

Figure 4 gives sketches of the tail surfaces and table I the main results of the tests. The investigation of the servo controls was carried out on the model surfaces Nos. 8, 9, and 10, and the results are given in table I. The choice of the schematized tail surfaces is explained by our original object in investigating servo controls, namely: comparison of experiment with theory. On figure 5 is shown a separate sketch of these models with servo controls and the main dimensions are indicated. The servo controls in the form of flaps extend along the entire span of the tail surface. For

the profile section we chose M-3 having 12 percent thickness as being one of the most widely used.

The dimensions were chosen as large as possible so as to improve the quality of the tests, particularly since all the tests essentially lead to the obtaining of hinge-moment coefficients and these coefficients, as is well known, are particularly sensitive to the scale effect. The three models differed from one another only as regards the ratio of control-surface area to tail-surface area. In our tests $\frac{S_{cs}}{S_t}$ has the following values: Tail surface No. 8; $\frac{S_{cs}}{S_t}$ = 0.6; No. 9: $\frac{S_{cs}}{S_t}$ = 0.5; No. 10: $\frac{S_{cs}}{S_t}$ = 0.4. There was thus included the entire practical range of variation of this ratio.

Servo controls of two sizes were prepared from brass and formed the trailing-edge portion of the section without departing from the outline of profile M-3. The ratio $\frac{S_{sc}}{S_t}$ for the large and small servo control had the following values: Small servo control, $\frac{S_{sc}}{S_t}$ = 0.065; large servo control, $\frac{S_{sc}}{S_t}$ = 0.08.

The servo controls were removable and could, if required, be removed from one surface and mounted on another. The following values of the ratio of servo-control area to the area of the main control were thus obtained:

Table II

Tail surface	$\frac{S_{cs}}{S_t}$	$\frac{S_{sc}}{S_{cs}}$	
		Small servo flap	Large servo flap
8	0.6	0.05	0.1075
9	.5	.06	.13
10	.4	.075	.16

There was thus obtained a range of from 5 to 16 percent of the area of the control surface.

Finally, the hinges of the main-control surfaces were constructed in such a way as to permit the variation of axial balance from 0 to 20 percent. Tail surface No. 9, which was selected by us as the basic one and on which extensive tests were made, was balanced 0, 10, 20, 23, and 26 percent. In the remaining cases, the balance consisted of 0, 10, and 20 percent of the area of the main control surface.

The test program was divided into three parts:

1) Tests on servo controls in the form of flaps.

2) Tests on servo controls with cut-outs.

3) Tests on servo controls mounted on outriggers behind the trailing edge.

The servo controls of the flap type are shown on figure 5 and formed flaps along the entire span of the trailing edge, or more properly speaking, the brass trailing edge could be deflected 30° to 40° up and down about hinges. For this type of tail surface, the tests were carried out on all three tail-surface models.

The servo controls with cut-outs are illustrated on figure 6 and are of the flap type except that instead of extending over the entire span the servo surface extends over only part of the span. These surfaces were formed out of the flap type servo-control surfaces in the following manner. The large servo-control flap was cut into three parts in such a manner that the center portion extended over half the span while the other two each extended over one-quarter span.

Tests were carried out with tail surface No. 9 and the large servo control surface, first with the outer portions deflected, the center remaining fixed and then with the center portion deflected and the outer portions remaining fixed. This enabled the effect of the arrangement of the servo-control surfaces along the span to be studied.

Finally, the servo controls mounted behind the trailing edge were made of the same sizes as the cut-out servo controls, i.e., they formed servo controls with six percent

of the area of the main tail surface No. 9 and were mounted behind the trailing edge of the main surface at distances of one, two, and three servo chords. Figure 7 shows the plan view and dimensions of this type of servo control.

The servo controls of the flap type were chosen as the basic type in our investigation and therefore the tests made on them were more extensive, making possible a complete study of the effect of the fundamental parameters of the servo-control surfaces on the action of the tail surface. The tests on the other two types had as their main object the investigation of the effect of the location of the servo control with respect to the span and chord of the main-control surface and therefore the tests on these were less extensive in character.

Due to the large dimensions of the models and the speeds of the order of 50 m/s, the Reynolds Number of the models tested attained a value from 1,200,000 to 1,500,000; the turbulence of the wind tunnel was defined by the critical sphere radius R_{cs} = 144,000 corresponding to a degree of turbulence ϵ = 1.82 percent.

The coefficients C_y, C_x, C_m, and C_h were determined in the usual manner on the wind-tunnel apparatus.

$$C_y = \frac{P}{\rho S_t V^2}$$

$$C_x = \frac{Q}{\rho S_t V^2}$$

$$C_m = \frac{M}{\rho S_t V^2 b_t}$$

$$C_h = \frac{M_h}{\rho S_{cs} V^2 b_{cs}}$$

The tests on the servo controls led essentially in the first place to the obtaining of curves of hinge-moment coefficients of the main-control surface $C_h = f(\delta)$ with

various servo areas and various degrees of balance for the determination of the "effectiveness of balance" of the servo control (under the term "effectiveness of balance" we mean the ratio of the hinge moment of the control surface with servo control to the hinge moment without servo control); and secondly, to the obtaining of curves of the lift force $C_y = f(\delta)$ for the determination of the loss in effectiveness of the control surface due to the servo surface. In addition, there were obtained curves of the equilibrium angles of deflection δ of the main control surface as a function of the angles of deflection θ of the servo control surface, i.e., the curves $\delta = f(\theta)$.

After applying all the corresponding corrections, there were determined the derivatives $\frac{\partial C_y}{\partial \alpha}$, $\frac{\partial C_y}{\partial \delta}$, $\frac{\partial C_h}{\partial \alpha}$, and $\frac{\partial C_h}{\partial \delta}$.

All these data are presented in table I. As we have already said, our object was to determine accurately the values of the derivatives for the purpose of finding rational analytical relations enabling the determination of the tail characteristics and the stability of the airplane.

3. EFFECTIVENESS OF THE TAIL SURFACES

a) Unbalanced and Balanced Tail Surfaces

The concept of effectivenss of tail surface is intimately connected with the force that the surface may develop for various flight conditions of the airplane. We shall therefore represent the effectiveness of the tail surfaces by the nondimensional coefficient C_n or more often by C_y since, within the small range of angles at which the tail surfaces usually operate, C_y barely differs from C_n.

Bringing an airplane into a position of equilibrium and effecting a change from this position is attained with the aid of a change in the angle of deflection of the control surface or a rotation of the entire tail surface. Hence, for a quantitative determination of the condition of equilibrium of the airplane and its stability, it is necessary to possess a knowledge of the change in C_y of the tail with change in angle of attack and angle of deflec-

tion of the control surface, i.e., of the value

$$dC_y = \frac{\partial C_y}{\partial \alpha} d\alpha + \frac{\partial C_y}{\partial \delta} d\delta \qquad (12)$$

In addition, a knowledge of the value of C_y itself is necessary as a function of the geometric form of the tail and of its location with respect to the airplane. For the value of C_y good results are given by the somowhat modified formulas of Toussaint for the case of a balanced tail surface and without cut-outs as generally obtained with horizontal tail surfaces

$$C_y = \frac{\partial C_y}{\partial \alpha} (\alpha^\circ_{true} + n\,\delta^\circ) \qquad (13)$$

where $n = \sqrt{\frac{S_{cs}}{S_t}}$ within the limits of the usual ratio of S_{cs} to S_t (of 0.3 to 0.6). The value of $\frac{\partial C_y}{\partial \alpha}$ is likewise well determined by the formula of Toussaint suitable for various types of tails. As is known, the relative thickness influences the value of this derivative but, in view of the small differences in thickness of tail surfaces, this correction may be neglected:

$$\frac{\partial C_y}{\partial \alpha} = \frac{0.0424\,\lambda}{1.73 + \lambda} \qquad (14)$$

Figure 8 illustrates this. As may be seen, the agreement of experiment with the formula is entirely satisfactory. It should be observed that there is a certain straining in the definition of the magnitude $\lambda = \frac{l^2}{S}$ in the case of a tail with cut-out where, following the usual method of computation, we obtain a value of λ larger than for a tail surface without cut-out. For tail surfaces with axial balance, a large number of which were investigated, we assume the following type of relation

$$C_y = \frac{\partial C_y}{\partial \alpha}\left[\alpha^\circ_{true} + n\delta^\circ\left(1 - 0.75\,\frac{S_{bal}}{S_{cs}}\right)\right] \qquad (15)$$

This expression is correct for tail surfaces without cut-outs for the $+15^\circ > \delta > -15^\circ$.

For $\alpha > 0$ and $15^\circ < \delta < 25^\circ$, as may be the case, for example, in computing the take-off, the value of $\frac{\partial C_y}{\partial \delta}$ [see equation (17) below] should be decreased by 40 to 50 percent, so that the effectiveness of the tail also decreases at these states.

A few tail surfaces with horn-type of balance were tested. These tests, moreover, were conducted in the smaller tunnel on comparatively smaller models, so that the proposed formula for the horn-type balance may serve only for orientation purposes. For horn-type balance

$$C_{y_t} = \frac{\partial C_y}{\partial \alpha}\left(\alpha^\circ_{true} + n\delta^\circ\right) \qquad (16)$$

within the range of δ from -20° to $+10^\circ$ for $\alpha > 0$ and $\delta = -10^\circ$ to $+20^\circ$ for $\alpha < 0$.

It should be noted that the formulas C_y for axial balance were obtained on the same tail surfaces and in the same wind tunnel as for the tail surface with horn-type balance. The repeated check at large values of R in the T-1 tunnel confirmed them, however.

Considerable importance attaches to the value $\frac{\partial C_y}{\partial \delta}$. An analytical expression for it may readily be obtained for tail surfaces with cut-outs and with and without axial balance

$$\frac{\partial C_y}{\partial \delta} = \frac{\partial C_y}{\partial \alpha}\, n\left(1 - 0.75\,\frac{S_{bal}}{S_{cs}}\right) \qquad (17)$$

A test check of this relation showed a satisfactory agree-

ment. It must be said that this check also shows the correctness of all the formulas given above, since formula (17) is the derivative (15).

According to the theory of errors, the probable relative error in computing $\frac{\partial C_y}{\partial \delta}$ is

$$r = 0.675 \sqrt{\frac{\Sigma(\Delta)^2}{n - 1}}$$

where Δ is the difference between the values of $\frac{\partial C_y}{\partial \delta}$ computed from (20) and that determined from tests, and n is the number of individual values of $\frac{\partial C_y}{\partial \delta}$ corresponding to the number of tail surfaces tested. The computation shows that the probable error r is about 4.8 percent.

It is interesting to bring out the effect of the form of leading edge of the control surface on the effectiveness of the tail surface. Tail surfaces Nos. 3, 4, and 5, differed in the form of leading edge. From the results of the tests and the data of table I it may be seen that the leading-edge form has practically no effect on $\frac{\partial C_y}{\partial \alpha}$ while it does have an effect on $\frac{\partial C_y}{\partial \delta}$ tail surface No. 3 giving a larger value for $\frac{\partial C_y}{\partial \delta}$ than Nos. 4 and 5, whereas formula (17) does not take this into account.

The series of points giving large deviations from the mean values of the effectiveness were probably the result of the deformation of the control surface, such a deformation being observed in particular with tail surface No. 7. These points may therefore be considered as being in error. In general, the deformation in deflecting the control surface may be considered as one of the main sources of error in the investigation of tail surfaces.

b. Effect of Cut-Outs on the Effectiveness of Control

We shall now attempt to evaluate the effect of cut-outs in the elevator on the effectiveness of the tail surface. As has already been said above, these cut-outs may amount to 20 to 25 percent of the control-surface area. It is true, as tests by Ackeret (reference 4) have shown, that these cut-outs at the after portion of the tail surface have a very small effect on the lift force. From this it follows directly that the computation of $\frac{\partial C_y}{\partial \alpha}$ with cut-outs in the tail surface does not lead to positive results, and the theoretical results obtained by Lotz (reference 5) show a loss in the lift very much larger than is obtained in tests.

Let us consider both derivatives $\frac{\partial C_y}{\partial \alpha}$ and $\frac{\partial C_y}{\partial \delta}$. The first one, in view of the small change in the lift as a result of the cut-outs, changes slightly. It may be remarked that there is a drop in $\frac{\partial C_y}{\partial \alpha}$ by 3 to 6 percent, and in only one case (with tail surface No. 11) does the drop amount to 12 percent. Without as yet proposing any quantitative criterion in the form of a rigorous functional relationship it may, for orientation purposes, be recommended that the value of $\frac{\partial C_y}{\partial \alpha}$ computed according to formula (14) be reduced by 3 to 6 percent for cut-outs of 8 to 15 percent of the control-surface area.

It is interesting to note that in the extensive Japanese investigations of wings with cut-outs (reference 6) for the cases of cut-outs behind the wings there were sometimes obtained even larger values of $\frac{\partial C_y}{\partial \alpha}$ than for complete wings. This phenomenon, not explained by the authors but observed in some of our tests (fig. 10), is evidently due to the rectangular edge of the cut-out producing a separation and formation of vortices and a suction of the boundary layer. This condition must be taken into account by the designer since unstreamlined rectangular cut-out edges, while only slightly increasing $\frac{\partial C_y}{\partial \alpha}$ produce a marked increase in the drag C_x of the tail or wing.

The effect of the cut-out can be somewhat more clearly expressed in the form of figure 11

$$\psi = \frac{\frac{\partial C_y}{\partial \delta} \text{ with cut-out}}{\frac{\partial C_y}{\partial \delta} \text{ without cut-out}} = 1 - 0.75 \frac{S_{\text{cut-out}}}{S_{cs}} \qquad (18)$$

i.e., with 10 percent cut-out there is a drop in $\frac{\partial C_y}{\partial \delta}$ of 7.5 percent. The test of Biechteler (reference 7) on a full-scale airplane in which tests the value of $\frac{\partial C_m}{\partial \delta}$ was measured pointed to a marked increase (up to 20 percent) in $\frac{\partial C_m}{\partial \delta}$ when the cut-outs (12.5 percent of S_{cs}) were eliminated (fig. 12).

The agreement of these results of Biechteler with the results of our tests is sufficiently good since in the absence of cut-outs there is obtained the expression*

$$\frac{\partial C_{m_a}}{\partial \delta} = + \frac{S_t L}{S_{cs} b} \left(\frac{V_x}{V}\right)^2 \frac{\partial C_{y_t}}{\partial \alpha} n = + \frac{S_t L}{S_w b_w} \left(\frac{V_x}{V}\right)^2 \frac{\partial C_y}{\partial \delta}$$

---

*This formula is obtained as follows. The moment of the entire airplane including the tail is equal to the moment resulting from the rotation of the elevator. For the unbalanced surface we thus have the expression,

$$C_{m_w} + C_{m_f} + \ldots + C_{m_t, \text{fixed cs}} + C_{m_t, \text{elevator}} = C_{m_a},$$

$$C_{m_t, \text{elevator}} = \sum C_{m_a}; \quad \sum C_{m_a} = \frac{S_t L}{S_w b_w} \left(\frac{V_x}{V}\right)^2 \frac{\partial C_{y_t}}{\partial \alpha} n\delta;$$

$$\frac{\partial C_{m_a}}{\partial \delta} = + \frac{S_t L}{S_w b_w} \left(\frac{V_x}{V}\right)^2 \frac{\partial C_{y_t}}{\partial \alpha} n$$

In the presence of cut-outs there enters into the value of $\frac{\partial C_m}{\partial \delta}$ the decreased area of the tail surface.

Thus the decrease in $\frac{\partial C_m}{\partial \delta}$ comes from two sources, namely the decrease in the coefficients $\frac{S_t L}{Sb}$ and the decrease in $\frac{\partial C_y}{\partial \delta}$ for the tail surface. If this circumstance is to be taken into account, it is necessary to introduce into the result obtained by Biechteler a correction for change in area of the tail surface. When this is done, we obtain a sufficiently good agreement of our formulas with the flight tests of Biechteler ($\psi_{comp} = 0.906$ and from Biechteler's tests 0.897).

Thus we have the following relations that take into account the effect of cut-outs on the tail characteristics:

1) $$\frac{\partial C_y}{\partial \alpha} = \frac{0.0424\,\lambda}{1.73 + \lambda} \qquad (14)$$

(it must be remembered that larger cut-outs somewhat lower this value)

2) $$\frac{\partial C_y}{\partial \delta} = \frac{\partial C_y}{\partial \alpha}\, n\left(1 - 0.75\,\frac{S_{bal}}{S_{cs}}\right)\psi \qquad (19)$$

3) $$C_y = \frac{\partial C_y}{\partial \alpha}\left[\alpha^\circ + n\delta^\circ\left(1 - 0.75\,\frac{S_{bal}}{S_{cs}}\right)\psi\right] \qquad (20)$$

c) Effectiveness of the Tail Surface with Servo Controls

The presence of servo controls reflects strongly on the values of $\frac{\partial C_y}{\partial \delta}$, i.e., on the slope of the curve $C_y = f(\delta)$. Naturally, in deflecting the servo control in a direction opposite to the deflection of the main control sur-

face, the effectiveness of the latter will more or less be reduced, depending on the basic parameters of the main- and servo-control surfaces.

In our tests for the determination of the effect of the servo control on the effectiveness of the main-control surface, we applied the following method. We obtained a series of curves $C_y = f(\delta)$ for various settings of the servo control varying δ from 0° to 20°. On figure 13 is given a series of such curves for tail surface No. 9 with 6 percent servo area for three values of the servo-control setting, namely, 0°, 10°, and 20°. With the aid of these curves, we constructed the curve $C_y = f(\delta)$ for a simultaneous deflection of the servo-control flap by the angle θ, which was in constant ratio with the angle of deflection δ of the main-control surface, i.e., $K = \frac{\theta}{\delta}$ remained constant. The curve $C_y = f(\delta)$ thus obtained with deflected servo tab was compared with the curve obtained without deflection of the servo tab. Thereafter, in conducting tests on the models of some airplanes, the test technique was very much simplified by the presence on the models of kinematic linkages between the servo- and the main-control surfaces (reference 8).

The method we had chosen made it possible to obtain an answer to the question of the effect of the servo control of the servo-balance type on the effectiveness of the main-control surface. In solving this same problem for servo controls proper, the method of conducting the tests would be different, as for example, the method used by Reid (reference 9), which consisted first in determining the relation $C_y = f(\delta)$ without servo tab and then determining the new relation with servo tab added, the latter being deflected by an angle which, for a given deflection of the main-control surface, assured a zero hinge moment. The latter method could also be applied in investigating servo controls of the balance type, but in our opinion, it is less suitable than the method we had chosen for a systematic investigation with the object of obtaining a definite connection between the loss in effectiveness of the main-control surface due to the presence of the servo tab and the various parameters of the tail surface. In any case, it is necessary to bear in mind that the results of the tests obtained by these two methods may be made comparable only after they have been brought into correspondence with each other.

The results obtained by us by the above method are given in figures 14 to 19 for all of the six arrangements of the servo- with the main-control surfaces. On each figure are given the curves $C_y = f(\delta)$ with undeflected servo tab ($\theta = 0$) and with deflected servo at $K = \frac{\theta}{\delta} = 1$; i.e., at such deflection of the servo tab for which the angles of deflection of the main- and servo-control surfaces were equal but of opposite sign. The dotted curves of figures 14 and 15 are for the same tail surface and servo control but unbalanced. From these curves it may be seen that axial balance has no effect on the loss in effectiveness of the main-control surface due to the servo tab but decreases the maximum lift coefficient $C_{y_{max}}$

A formula that takes account of the loss in effectiveness due to the servo tab may be proposed of the following form:

$$\Delta C_{y_{sc}} = - \frac{7.2}{1 + \lambda_t} \frac{\partial C_y}{\partial \delta} \frac{S_{sc}}{S_{cs}} \left(1 + \frac{t}{b}\right) K(1 - 0.0025 \delta^2 K) \delta \qquad (21)$$

where t is the mean servo chord

b, the chord of the main-control surface at the position of the mean servo chord.

The value $K = \frac{\epsilon}{\delta}$ (coefficient of kinematic linkage) enters as an absolute factor in the formula. Table III below gives the values of $\Delta C_{y_{sc}}$ obtained with the aid of this formula for $\delta = 10^\circ$ and $K = 1$, and those obtained directly from tests on all six combinations of servo- and main-control surfaces Nos. 8, 9, and 10.

Table III

$\frac{S_{sc}}{S_{cs}}$	0.05	0.06	0.075	0.1075	0.13	0.16
$\frac{\partial C_y}{\partial \delta}$	0.0219	0.0200	0.0179	0.0219	0.0200	0.0179
$\Delta C_{y_{sc}}$ (comp.)	-.0138	-.0152	-.0173	-.0321	-.0353	-.0399
$\Delta C_{y_{sc}}$ (exper.)	-.013	-.015	-.017	-.035	-.035	-.04

The results of the comparison may be considered entirely satisfactory. This loss in effectiveness of the main-control surface must therefore be taken into account in the computation of the static stability in determining C_{m_z} due to the tail surface at various deflections of the main-control surface.

In recent times on all high-speed airplanes are mounted tail surfaces with fixed stabilizer with the object of obtaining the smoothest possible connection of the tail portion of the fuselage to the tail surfaces and hence a better flow and reduced parasite drag. In such cases a servo-control tab selected from the condition of limiting deflection in landing may be conveniently divided into two parts, one of them in the form of a balancing tab, the other controlled from the pilot's cabin to be held in reserve as a trimming tab in the case of insufficient balance from one of the servo-control tabs. In landing, both servo-control tabs work together in one direction relieving the pressure on the stick. For those flight conditions, however, where such large balance is not required, the servo balance operates either by itself or in conjunction with the trimming tab deflected by a small angle required to obtain normal pressure on the control stick. With the aid of such a combination of servo-control and trimming tabs, there is more conveniently obtained zero pressure on the stick for any condition of steady level flight with fixed stabilizer; i.e., with the aid of a trimming tab, it is possible to so regulate the control in flight that flight can be accomplished with stick free.

In the presence of a trimming tab the change in lift C_y of the control surface may be taken into account by the following empirical formula:

$$\Delta C_{y_{tab}} = \frac{7.2}{1 + \lambda_t} \frac{\partial C_y}{\partial \delta} \frac{S_{tab}}{S_{cs}} \left(1 + \frac{t}{b}\right) (1 + 0.0025\delta_{cs}\theta_{tab})\theta_{tab} \quad (22)$$

This formula is obtained from formula (21) by replacing K in the latter by $\frac{\theta}{\delta}$.

Thus the effectiveness of the tail expressed by formula (20) modified to take account of the loss in effectiveness due to the servo control tab is given by the following formula:

$$C_y = \frac{\partial C_y}{\partial \alpha}\left\{\alpha^\circ + n\left(1 - 0.75\frac{S_{bal}}{S_{cs}}\right)\psi - \left(\delta^\circ - \frac{\Delta C_{y_{sc}}}{\frac{\partial C_y}{\partial \delta}} + \frac{\Delta C_{y_{tab}}}{\frac{\partial C_y}{\partial \delta}}\right)\right\} \quad (23)$$

where $\Delta C_{y_{sc}}$ and $\Delta C_{y_{tab}}$ are taken from formulas (21) and (22).

The servo controls with cut-outs, as has already been stated, were the same as those of the flap type except that they did not extend over the entire span but only over part of it. To explain the effect of the spanwise position of the servo-control tab, the servo controls in our tests were placed first at the center and then outboard of the span (fig. 6). On figures 20 and 21 are given curves of effectiveness of the main control surface with and without deflection of the servo-control tab. Examination of these curves shows that the different location of the servo-control tab along the span has no effect on the loss in effectiveness; in both cases we have the same loss in effectiveness. From the point of view of the loss in effectiveness of the main-control surface, it is therefore entirely immaterial where the servo-control tab is located with respect to the span for a constant-chord control surface. In the case of a control surface with variable chord, it is naturally more advantageous to place the servo-control tab at the position of maximum chord of the main-control surface.

A comparison of figures 20 and 21 with figures 14 and 15, which show the curves of effectiveness of the same tail surfaces with servo controls of the flap type having the same areas, shows an increased loss of effectiveness for the servo tabs with cut-outs. At the same time, however, we see in all cases a good agreement of the test results with the values of ΔC_y obtained by formula (21) for $\delta = 10^\circ$ and $K = 1$. The results are given in table IV.

Table IV

	Type of servo		
	flap	center	outboard
$\Delta C_{y_{sc}}$ from formula	0.0152	0.016	0.016
$\Delta C_{y_{sc}}$ from tests	.015	.0158	.0158

This increased loss of effectiveness in the case of the servo tabs with cut-outs as compared with the servo control

of the flap type is a result of the decrease in span of the servo-control tab, and this is taken into account in formula (21) by the factor $\left(1 + \frac{t}{b}\right)$. Hence from the point of view of decrease in effectiveness of the main-control surface, it is advantageous to give the servo-control tab a greater span.

The servo controls that were mounted at some distance from the trailing edge were of the same size as regards area as the flap type of servo No. 9 with the small servo area and the servo tabs with cut-outs, i.e., the servo area was six percent of that of the main-control surface. It was thus possible to compare the effectiveness of the servo controls of the three types. The outrigger types were mounted at various distances from the trailing edge starting with "zero distance" where the leading edge of the servo tab coincided with the trailing edge of the main-control surface and ended with a projected distance of three chords, i.e., when the leading edge of the servo-control tab was at a distance from the trailing edge of the main-control surface equal to three servo-control chords. The servo-control tabs were of rectangular plan form and aspect ratio $\lambda = 6$.

As regards the loss in effectiveness of the main-control surface due to the servo-control tab, it may be seen from figure 22 that this loss in projecting the servo-control tab out from the trailing edge reduces to a minimum and practically need not be taken into account. This is due to the fact that in the case of the servo control of the flap type and type with cut-outs a deflection of the servo control is equivalent to a change in the camber of the main-control surface, an effect which shows up strongly on the change in its aerodynamic characteristics. In the case of the outrigger-type, servo controls, however, any decrease in the effectiveness of the main-control surface is due to the interference effect between the servo- and main-control surfaces as in the case of a tandem-type wing or biplane cellule.

Thus, servo-control tabs which are projected out from the trailing edge have a clear advantage over other types as far as their effect in reducing the effectiveness of the main-control surface is concerned. This advantage, however, is hardly offset by the structural complications and greater tendency to vibration introduced by such a system and also, it must be supposed, by the greater drag due to the projecting brackets. From these considerations it

is hardly probable that this type of servo-control tab will receive any wider application than it has received up to this time. These considerations led us to limit the number of tests on this type and the tests conducted are therefore quite insufficient for deriving any basic formulas for the outrigger type servo controls. The formulas given for computing the effectiveness of the servo control and the loss in effectiveness of the main-control surface due to the other two types of servo, i.e., formulas (22) and (23), are not suitable for the outrigger type of servo control.

4. EFFECT ON THE DRAG

The question of tail-surface drag is beginning to attract more and more attention in connection with the increasing speeds of airplanes. We have already pointed out one of the factors connected with a decrease in drag, namely, the application of sections with sharpened leading edge. The advantage in this case will show up particularly at large speeds where $Ba > 0.4$ (reference 10).

It was very interesting to note the role of cut-outs in increasing the drag of the tail surfaces. Figure 24 shows how considerable may be the increase in drag with increase in amount of cut-out. The curve gives the upper limit of the increase in drag obtained for tail surfaces with straight cut-out edges (fig. 10a) tail surface No. 12, and the surfaces tested in the Japanese laboratories. A change in the form of the cut-out obtained by giving a streamlined form to the trailing ege (fig. 10b) gave for the same tail surface, No. 12, a considerable decrease in drag. (See reference 6*.)

An analysis of the polar of tail surface No. 12 (fig. 25) shows that cut-outs have an effect on the profile drag and affect the induced drag only by the usual amount through the aspect ratio λ (without additional corrections).

Examination of figure 25 shows that the change in profile drag of the tail surfaces with increase in cut-out remains almost constant over the entire range of the polar, a fact which indicates the correctness of the method of defining λ by the ratio $\frac{l^2}{S_{true}}$. If we had considered that

*The curve on our figure was obtained by a work-up of the experimental data given in this report.

the cut-out had not changed λ, we would have received at large angles of attack a sharp decrease in the profile drag and this would not have corresponded to the physical phenomenon. On figure 26 are shown the curves of drag for tail surfaces with various forms of control surface loading edge (Nos. 3, 4, 5).

5. CENTER OF PRESSURE

As is known, in the computation of stability as normally conducted in design offices, the center of pressure of the tail surface is considered as lying either on the hinge axis of the elevator or at some other point of the tail-surface chord as, for example, at one third chord. It was interesting in testing the models to investigate how these rough approximations corresponded to the actual state of affairs. With this idea in mind, we proceeded as follows. Considering the work of each tail surface, we may divide the lift coefficient C_y of the tail surface into two parts, a part C_{y_α} depending only on α at $\delta = 0$, and a part C_{y_δ} depending only on the deflection of the control surface for some constant angle α_t.

Under these conditions, the moment of the tail surface may be written in the following form

$$C_m = m_\alpha C_{y_\alpha} + q_\delta C_{y_\delta} \qquad (24)$$

In this expression the value $m_\alpha = \frac{\partial C_m}{\partial C_y}$ at undeflected elevator is the same as $\frac{\partial C_m}{\partial C_y}$ for a wing which has the same plan form as the tail surface. This value may be found beforehand analytically knowing the plan form of the tail surface (reference 11).

In the case where wind-tunnel tests on the model tail surfaces are available, the value of $m_\alpha = \frac{\partial C_m}{\partial C_y}$ may be directly obtained from the test curves. The value of m_α

does not depend on the profile section and practically does not vary as a result of cut-outs at the trailing edge, as may be seen from the tests on model 12 (fig. 27). The coefficient C_{y_α} is the C_y of the tail surface for $\delta = 0^\circ$.

$$C_{y_\alpha} = \frac{\partial C_y}{\partial \alpha^\circ} \alpha^\circ$$

The second term on the right of equation (24) is made up of q_δ and C_{y_δ} where C_{y_δ} is a function only of δ

$$C_{y_\delta} = \frac{\partial C_y}{\partial \delta} \delta^\circ$$

$$C_y = C_{y_\delta} + C_{y_\alpha}$$

and $q_\delta = \frac{\partial C_m}{\partial C_y}$ oscillates about a mean value of about 0.48. The probable relative error in determining the value of q_δ is 4.5 percent.

Thus the moment coefficient of the tail surface and hence also the position of the center of gravity may be computed from the formula

$$C_m = m_a \frac{\partial C_y}{\partial \alpha} \alpha + 0.48 \frac{\partial C_y}{\partial \delta} \delta \qquad (25)$$

$$\frac{x}{b} \cong \frac{C_m}{C_y} = \frac{m \frac{\partial C_y}{\partial \alpha} \alpha + 0.48 \frac{\partial C_y}{\partial \delta} \delta}{\frac{\partial C_y}{\partial \alpha} \alpha + \frac{\partial C_y}{\partial \delta} \delta} \qquad (26)$$

The method just explained enables a preliminary rough computation to be made of the moment coefficient C_m and a more accurate location of the center of pressure on the tail

surface. Although the effect produced by the change in lever arm of the force acting on the tail surface is small even "small differences" in the moment of the entire airplane and the balancing moments arising from the deflection of an elevator of a modern airplane with small degree of stability require as great accuracy of computation as possible if it is desired to obtain agreement between the computed and actual performance. For a comparison of the various methods of finding the center of pressure on the tail surface stability computations were made on one of the airplanes with a small degree of stability. The computation was carried out by four methods.

1) By taking into account the actual coefficients C_y, C_x, and C_m, and the actual lever arms of the forces - the "accurate" method.

2) By the method proposed by us.

3) By considering C_{y_t} located on the hinge axis.

4) By considering C_{y_t} located at 25 percent chord in the airplane plane of symmetry.

By computing C_{m_z}, we may set up a table giving the ratio $\frac{C_{m_{z_t}}}{C_{m_{z\ I}}}$. This ratio may be taken as a measure of the perfection of the method

Table V

α^o	0	4	8	12
$\frac{C_{m_{z\ II}}}{C_{m_{z\ I}}}$	1.0125	1	1.02	1.019
$\frac{C_{m_{z\ III}}}{C_{m_{z\ I}}}$	-	1.078	1.078	1.065
$\frac{C_{m_{z\ IV}}}{C_{m_{z\ I}}}$	-	.939	.988	.978

The method proposed thus appears to be more accurate than those by which the center of pressure is located at 25 percent chord or on the hinge axis. It may be said in passing that it may be considered more correct to locate the center of pressure at 35 percent chord.

6. FORCES IN DEFLECTING THE ELEVATOR

a) Unbalanced and Balanced Tail Surfaces

As is known the questions of stability and balance of the airplane are intimately connected with those of the forces which arise in controlling the airplane. The mutual relation between these problems is particularly strong when considering the behavior of the airplane with stick free as was pointed out in the first section of our article. The possibility of computing the hinge moments of the control surface is thus essential not only from the point of view of determining the control forces but also from that of evaluating the stability and balance of the airplane.

The control force T is expressed in the following form

$$T = K_o M_h = K_o C_h \rho S_{cs} v^2 b_{cs} \qquad (27)$$

where K_o is the coefficient of transmission from control surface to control stick. Hence to find the control force it is necessary to know the value C_h, which may be expressed by

$$C_h = \frac{\partial C_h}{\partial \alpha} \alpha_t + \frac{\partial C_h}{\partial \delta} \delta_{cs} = K_1 \alpha_t + K_2 \delta_{cs} \qquad (28)$$

It will be our object to bring out the relation between the values $\frac{\partial C_h}{\partial \alpha}$ and $\frac{\partial C_h}{\partial \delta}$ and the basic parameters of the tail surfaces. It is first necessary to make a few remarks. Since our tests were conducted on tail surfaces with axial balance, without balance and with servo balance, we can give quantitative descriptions of only these three types of tails.

The second remark refers to the increase in accuracy in the determination of the value of the axial balance. In a detailed consideration of the problem it appeared useful to define the axial balance as shown on figure 28. It thus appeared that certain tail surfaces which were considered as unbalanced by their designers had 3 to 7 percent of axial balance.

The third remark relates to the following consideration. The determination of the hinge moments in the laboratories is an operation that is less accurate than the determination of the effectiveness so that the coefficient C_h for even large tail models is much less accurately determined than the lift coefficient C_y. For this reason the same accuracy cannot be expected of the relations expressing the hinge moments as of those expressing the lift coefficient C_y.

As may be seen from the given curves C_h is essentially a linear function of δ for $+15 > \delta > -15$, so that there is no difficulty in finding the slope $\partial C_h/\partial\delta$. Referred to the mean geometric chord of the control surface, we obtain the curve shown on figure 29, which enables $\frac{\partial C_h}{\partial \delta}$ to be expressed by the following relation which agrees closely with that proposed by B. F. Goncharov (reference 12) for the case of axial balance:

$$\frac{\partial C_h}{\partial \delta} = 0.00573 \left(1 - 3.33 \frac{S_{bal}}{S_{cs}}\right) \qquad (29)$$

This magnitude depends on the form of leading edge of the control surface and of the tip of the stabilizer, on the amount of cut-out, and on a number of other tail-surface parameters. We therefore observe on the curves a rather large amount of scattering of the points, which arrange themselves along a family of straight lines. The extreme limiting coefficients before the parenthesis in formula (29) will be 0.00675 and 0.0047. Thus in taking the coefficient as 0.00573, we make a possible error of the order of 15 percent. If we take for $\frac{\partial C_h}{\partial \delta}$ the straight line with slope 0.00573 as the basic one, then computation of the

probable relative error gives the value r = 9.75 percent. This figure is considerably reduced if the coefficient is chosen so as to take into account the tail characteristics as will be seen below.

It is as yet difficult to speak of a greater accuracy in determining the effect of the tail characteristics on the change in $\frac{\partial C_h}{\partial \delta}$ since on the one hand the probable error is large and on the other the phenomenon is so complicated that a detailed analysis at the present time is laborious. On the basis of the available material, it is possible to estimate roughly the change on $\partial C_h/\partial \delta$ which is brought about by cut-outs. From a comparison of the results of the tests it is evident that a cut-out decreases $\frac{\partial C_h}{\partial \delta}$, the relation between the latter and $S_{cut\text{-}out}/S_{cs}$ being shown on figure 30. This decrease is to be expected since the loading is reduced and the lever arm of the hinge moment decreases as a result of the forward displacement of the center of pressure.

Of the other elements of the tail surface that have an effect on $\frac{\partial C_h}{\partial \delta}$, there may be mentioned the form of the leading edge of the control surface. The blanketed leading edge in the presence of axial balance gives an increase in $\frac{\partial C_h}{\partial \delta}$ since the balance is not completely effective being screened by the trailing edge of the stabilizer. When the trailing edge of the stabilizer is made sharp, the effectiveness of the balance increases and the slope decreases (compare tail surfaces 3 and 4).

Guided by these data we may indicate the probable limits for the curve of $\frac{\partial C_h}{\partial \delta}$ against S_{bal}/S_{cs}. For tail surfaces without cut-outs and with sharp leading edge of the control surface shielded by the stabilizer, it is necessary to take the upper values for the intercept of the $\frac{\partial C_h}{\partial \delta}$ curve, namely, 0.0057 - 0.0067. On the other hand, for

tail surfaces with unshielded leading edge and with cut-outs, the value of the intercept must evidently be chosen within the range 0.0047 - 0.0057.

The other derivative determining the value of the hinge moment, namely: $\frac{\partial C_h}{\partial \alpha}$ is obtained from tests with even greater difficulty than $\frac{\partial C_h}{\partial \delta}$ since the method itself of finding this derivative from the test curves determines a large probable error. Figure 31 gives the dependence of the derivative $\frac{\partial C_h}{\partial \alpha}$ on $\frac{S_{cs}}{S_t}$ and $\frac{S_{bal}}{S_{cs}}$. The analytical form of this relation for a control surface with unsharpened leading edge is

$$\frac{\partial C_h}{\partial \alpha} = \left(0.00538 - 0.0166 \frac{S_{bal}}{S_{cs}}\right) \frac{S_{cs}}{S_t} \qquad (30)$$

The curves on the figure are interpolated straight lines. The points correspond to the values K_s for the tail surfaces tested. The values of S_{bal}/S_{cs} for all tail surfaces may be taken from table I. The probable relative error obtained from a comparison of the computed values of $\frac{\partial C_h}{\partial \alpha}$ and those obtained experimentally is 33.7 percent.

The accuracy in the determination of $\frac{\partial C_h}{\partial \alpha}$ is less than in that of $\frac{\partial C_h}{\partial \delta}$ but this defect is compensated by the fact that the term $\frac{\partial C_h}{\partial \delta}$ in the general expression for C_h is of considerably less importance than the term $\frac{\partial C_h}{\partial \alpha}$.

As regards the change in $\frac{\partial C_h}{\partial \alpha}$ with modification of the tail surface, it is difficult to draw any conclusions as to the effect of cut-outs on account of the inconsistencies involved. The greatest value of the derivative

$\frac{\partial C_h}{\partial \alpha}$ is given by a dulled leading edge (tail surface No. 5). This value of 0.0008 comes nearest to that determined by formula (30), namely, 0.00095. A sharpened nose of the control surface (tail surface No. 3 or No. 4) gives a larger decrease in this derivative.

Thus, the mean value of C_h for the unbalanced and balanced tail surfaces is completely expressed by the relation

$$C_h = \left[0.00573\left(1 - 3.33\frac{S_{bal}}{S_{cs}}\right)\right]\delta^\circ + \left[\left(0.00538 - 0.0166\frac{S_{bal}}{S_{cs}}\right)\frac{S_{cs}}{S_t}\right]\alpha^\circ \qquad (31)$$

b) Tail Surfaces with Servo-Control Tabs

The procedure for obtaining the curves of hinge-moment coefficients with servo-control tabs was the same as for obtaining the curves of effectiveness of main-control surface. A family of curves, $C_h = f(\delta)$, with θ the setting of the servo-control tab as parameter was obtained. The curves are shown on figure 32. From these curves were constructed the curves $C_h = f(\delta)$, taking into account the servo-tab deflection for the ratio $K = \frac{\theta}{\delta}$ equal to unity. These curves were obtained for all the servo controls. On figures 33-38 are given curves of the hinge-moment coefficients as a function of δ for various amounts of balance. For each balance condition there are given two curves of hinge-moment coefficients: one without servo-tab deflection and one with servo-tab deflection for $K = 1$.

Formula (28) may be written in the form

$$C_h = K_1 \alpha_t + K_2 \delta = C_{h_1} + C_{h_2}$$

where α_t is the angle of attack of the tail surface and δ the angle of deflection of the control surface. From the curves given, an expression may be obtained for the coefficient K_2 which should consist of three terms, namely,

$$K_2 = \frac{\partial C_h}{\partial \delta} = \left(\frac{\partial C_h}{\partial \delta}\right)_0 - \Delta_1 \frac{\partial C_h}{\partial \delta} - \Delta_2 \frac{\partial C_h}{\partial \delta} \qquad (32)$$

where $\left(\frac{\partial C_h}{\partial \delta}\right)_0$ is the value of $\frac{\partial C_h}{\partial \delta}$ without any balance, $\Delta_1 \frac{\partial C_h}{\partial \delta}$ is the decrease in the value of $\frac{\partial C_h}{\partial \delta}$ due to balancing and, finally, $\Delta_2 \frac{\partial C_h}{\partial \delta}$ is the decrease in the value of $\frac{\partial C_h}{\partial \delta}$ due to the servo tab. The expression for the first two terms for K_2, i.e.,

$$\left(\frac{\partial C_h}{\partial \delta}\right)_0 - \Delta_1 \frac{\partial C_h}{\partial \delta}$$

has already been met with before (formula (31)).

The effect of the servo-control tab in decreasing the value of C_{h_2}, which we denoted in formula (32) by $\Delta_2 C_{h_2}$ was obtained from the same curves of figures 33-38 and may be expressed by a formula very similar to the one which takes account of the loss in effectiveness (21)

$$\Delta_2 C_{h_2} = - \frac{7.5}{1 + \lambda_t} \frac{\partial C_y}{\partial \delta} \frac{S_{sc}}{S_{cs}} \left(1 - \frac{t}{b}\right) (1 - 0.0025\, \delta^2 K)\, \delta \qquad (33)$$

In table VI below are given the values of $\Delta_2 C_{h_2}$, computed by this formula and also the values obtained from tests for $\delta = 10^\circ$.

Table VI

$\frac{S_{sc}}{S_{cs}}$	0.05	0.06	0.075	0.110	0.130	0.160
ΔC_{h_2} (comp.)	.012	.014	.0155	.027	.0285	.030
ΔC_{h_2} (exper.)	.010	.014	.017	.032	.030	.30

With regard to $K_1 = \frac{\partial c_h}{\partial \alpha}$ it should be observed that the presence of a servo-control tab does not change its value and this circumstance, which makes the servo balance differ considerably from other types of balance, shows up very disadvantageously on the stability of the airplane in flying with stick free, there being obtained a lowering in the stability. The deflection of the unbalanced control surface in flight with stick free determined from the condition of zero value of the hinge moment according to formula (7)

$$\delta = - \frac{K_1}{K_2} \alpha_t \qquad (7)$$

hardly changes as a result of axial balance since the coefficients K_1 and K_2 change at the same rate with increase in the amount of balance as a result of which their ratio $\frac{K_1}{K_2}$ may, for a tail surface of a given type, be considered constant. In the case of servo balance, however, the value of δ, as a result of the increase in K_2 at constant K_1, sharply increases and therefore the stability of the airplane in stick-free flight is relatively lower as compared with the stability with free unbalanced controls. This fact must be taken into account in providing the elevator with servo balance, since with a small reserve of stability with free, balanced controls the airplane may become unstable in flying with stick free.

In our present work no special investigation of the effect of a change in angle of attack of the tail surface on the action of the servo-control tab was undertaken in view of the fact that the data available on other tail surfaces have shown that a change in the angle of attack up to 12° has no effect on the effectiveness of the balance due to the servo control. The angle of attack of the tail surface generally does not exceed 12° and for this reason we did not find it necessary to conduct a special investigation on our tail surfaces but decided to make use of the material already available on other tail surfaces.

On figure 39 are given curves of elevator hinge moment coefficients for tail surface No. 14 with 6.44 percent servo-control tab for angles of attack of the tail plane $\alpha_t = 0^\circ$ and $\alpha_t = 10^\circ$. The curves of the hinge moment coeffi-

cients in both cases run equidistant from each other. The same may be observed on two other curves. Figure 40 shows the hinge-moment coefficients for tail surface No. 11 with 10 percent servo and figure 41 shows the curves for No. 12 with 7 and 10-percent servo. On the latter figure (41), there may be observed a change in the effectiveness of the balance only at a tail angle of attack equal to 14°, no change being observed up to 12°. Finally, on figure 42 are shown the curves of effectiveness of the tail, i.e., the curves $C_y = f(\delta)$ for the various values of the angle of attack α° with the servo deflection taken into account. These curves also likewise run parallel within their linear ranges.

It may be considered that a change in the tail angle of attack has no marked effect on the operation of the servo-control tab up to 12° and hence no corrections have been made in our formulas for change in angle of attack. Consequently, the general formula for the hinge moment taking into account axial balance and servo control may be written thus:

$$C_h = 0.00573\left(1 - 3.33\frac{S_{bal}}{S_{cs}}\right)\delta^\circ + \Delta_s C_{h_s} + \left[\left(0.00538 - 0.0166\frac{S_{bal}}{S_{cs}}\right)\frac{S_{cs}}{S_t}\right]\alpha^\circ \qquad (34)$$

where $\Delta_s C_{h_s}$ is taken from formula (33).

Where there is a trimming tab the hinge-moment coefficient changes by an amount determined by the formula

$$\Delta_s{}'C_{h_s} = \frac{7.5}{1+\lambda_t}\frac{\partial C_y}{\partial \delta}\frac{S_{tab}}{S_{cs}}\left(1 - \frac{t}{b}\right)(1 + 0.0025\delta_{cs}\delta_{tab})\theta_{tab} \qquad (35)$$

The formula for the hinge moment that takes into account axial balance, servo control, and trimming tabs, may be written as follows:

$$C_h = 0.00573 \left(1 - 3.33 \frac{S_{bal}}{S_{cs}}\right)\delta^\circ + \Delta_2 C_{h_2} + \Delta_2' C_{h_2} + \\ + \left[\left(0.00538 - 0.0166 \frac{S_{bal}}{S_{cs}}\right)\frac{S_{cs}}{S_t}\right]\alpha^\circ \qquad (36)$$

In formula (33) as in formula (21) there enters the factor $K = \frac{\theta}{\delta}$, i.e., the coefficient of kinematic linkage, which must be chosen in such a manner that the servo control is effective over the entire range of deflection of the main control surface. From figures 33-38, we may see that the servo tabs remain effective only up to a certain limiting servo deflection θ beyond which any further deflection remains entirely ineffective. On the same curves it may be observed that a decrease in the slopes of the hinge-moment curves due to the servo control occurs up to about 15°, beyond which the hinge-moment curves with servo run parallel to the corresponding curves without servo.

This is particularly clearly seen on the curves of equilibrium angles of the main and servo surfaces. The latter curves were obtained simultaneously with the curves $C_h = f(\delta)$ during the hinge-moment tests. The method of obtaining them was as follows. For a given angle of attack α and given servo deflection θ there was measured for the deflection δ of the main-control surface for which the moment of the air forces acting on the system composed of the main and servo surfaces, was equal to zero. By varying the servo angle θ from 0 to 40° there was obtained the "floating angle" curve $\delta = f(\theta)$ for a given angle of attack α. Such curves were obtained for all of the six servo arrangements with various degrees of axial balance, i.e., to each curve $C_h = f(\delta)$ of figures 33-38 there corresponds the floating-angle curve $\delta = f(\theta)$. The latter are given on figures 43-48.

As may be readily observed on examination of these curves, the servo controls are effective only within the relatively small range of servo deflection from 10° to 15° beyond which the curves have a very small slope, which is the same for all the servo controls independent of their dimensions, whereas in the range of effectiveness of the servo control the slopes of the curves increase almost

proportional to the increase in servo area. The value of $\frac{\partial\delta}{\partial\theta}$ is a measure of the sensitiveness of the main-control surface to deflection of the servo surface. Where there is axial balance the sensitiveness of the main-control surface increases with particular sharpness near the limit of balance, i.e., from 20- to 30-percent axial balance. On figure 44, for example, which gives the curves for 6 percent servo-control tab, there is the same increase in $\frac{\partial\delta}{\partial\theta}$ in varying the balance by 3 percent from 20 to 23 percent as in changing the balance by 10 percent from 10 to 20 percent.

A further increase in the degree of balance has a still greater effect on the increase in the sensitiveness of the main-control surfaces but, on the other hand, decreases the range of servo deflections up to 10 percent. With further deflection of the servo controls, the sensitiveness drops sharply to zero, i.e., the angle of deflection of the main control surfaces does not increase. Thus the axial balance increases the sensitiveness of the main surface to deflection of the servo surface but decreases the limits of effectiveness of servo deflection from 15° to 10°.

Guided by the foregoing remarks with regard to the equilibrium angle curves, it is always possible to select in any given case such a value for the coefficient of kinematic linkage K as would assure a complete utilization of the servo control for the entire range of deflection of the main-control surface.

For the limiting allowable servo deflection, there may be taken the value 15°. The value of $\delta_{max.}$ however, is determined from a computation of the longitudinal static stability and controllability as the limiting elevator deflection required for landing. Thus the value of the linkage coefficient K is determined from the following formula

$$K = \frac{15}{\delta_{max}} \qquad (37)$$

which gives the limiting value for K. A larger value than this for K cannot be taken since in that case the

servo-control surface will have exhausted its effectiveness before the main-control surface is deflected to its limiting position. A smaller value for K than that given by the above formula is disadvantageous since this will give a greater loss in effectiveness of the main-control surface.

On figure 49 are given curves of hinge-moment coefficients of tail surface No. 9 with cut-out servo tab. It may be seen from these curves that a servo tab placed outboard of the span is more effective than one placed at the center of the span, in the sense that it decreases the hinge moment control force. Comparing the servo with cut-out with the servo of the flap type (fig. 34), it may be said that the latter is more effective in decreasing the hinge moment, a fact that is again explained by the difference in the ratio of servo chord to main-control-surface chord and is taken into account in formula (33) by the factor $(1 - t/b)$; i.e., by the change in the servo tab aspect ratio. The values of $\Delta_2 C_{h_2}$ as obtained from test and as computed from formula (33) for a cut-out servo (at center span) are the same and equal to 0.017 for $\delta = 10^\circ$. Consequently, also as regards maximum effectiveness of balance, it is necessary to give the servo tabs as large an aspect ratio as possible. If it is not possible for structural reasons to give the servo surface the form of a flap, then it is desirable, in order to increase its effectiveness, to make use of the "tip effect" by placing it along the end of the span, provided such a location does not possibly give rise to vibration.

Figure 50 shows curves of equilibrium angles $\delta_c = f(\theta)$ for the cut-out type of servo control. Comparing these with the curves on figure 44, i.e., with those for the flap type, we may observe a complete correspondence with the hinge-moment curves, i.e., a greater effectiveness of the outboard servos and a loss in effectiveness of the cut-out types due to decreased aspect ratio.

Figure 51 shows hinge-moment coefficient curves $C_h = f(\delta)$ without servo tabs and with outrigger servo tabs for $K = 1$. It may be seen from these curves that the hinge-moment coefficients with undeflected servo increase as the projected distance from the trailing edge is increased. This is explained by the fact that for the undeflected condition of the servo, the latter produces a moment in addition to that of the main-control surface. As the distance of the servo from the trailing edge is increased, the lever arm of the servo tab with respect to the axis of the main-control surface increases and hence there arises a harmful additional hinge moment when the

servo tab is undeflected. With the servo tab deflected, the effectiveness of the balance also increases with increase in distance from the trailing edge.

Thus from the point of view of effectiveness of the servo balance, i.e., decrease in the hinge moments, it is entirely immaterial how much to carry the servo tab out behind the trailing edge. For the same servo tab and the same value of K at any distance we have the same value of the hinge moment C_h. Hence the value of C_h does not depend on the distance for the outrigger type of servo flaps.

Comparing figure 51 with figures 49 and 34 in which are given the curves $C_h = f(\delta)$ for the cut-out and flap type of servo controls it may be seen that the slopes of the curves with the servos of all three types are very nearly the same and have a mean value of 0.004, somewhat less for the cut-out and flap type and somewhat more for the outrigger type. The latter type compared to the other two types therefore has the advantage that it remains effective up to a large deflection angle.

Figure 52 shows the equilibrium-angle curves for an outrigger servo tab. The value of $\frac{\partial \delta}{\partial \theta}$, i.e., the sensitiveness of the main-control surface to deflection of the servo surface decreases at first with increase in distance from the trailing edge and then somewhat increases. For a distance of 1-2 chords, for example, the value of $\frac{\partial \delta}{\partial \theta}$ is less than in the case of zero distance away, and in the case of a servo control of the flap and cut-out type, at a distance of 3 chords the value of $\frac{\partial \delta}{\partial \theta}$ increases somewhat for small values of δ and then decreases again. The range of angles at which the outrigger type of servo control retains its effectiveness increases as compared with the other types, and has a mean value of 20°-25°. The same phenomenon may be observed on the curves of figure 51 giving the curves of hinge moment coefficients for the outrigger servo tabs.

7. CONCLUSION

In the solution of a number of problems on the stability and controllability of airplanes, there arises the necessity for knowing the characteristics of the tail surfaces of the types in common use today. Of these characteristics, the most important are the effectiveness and hinge moments of the tail surfaces. As has been shown in the present paper, there exists the possibility of determining these characteristics by the formulas obtained with a degree of accuracy sufficient for the purposes of a preliminary computation. These formulas take into account a number of fundamental tail characteristics. One of these is the presence of cut-outs on the control surface (it is true that in recent times designers with complete justification try to avoid these cut-outs). A method has here been presented of estimating the effect of these cut-outs on the tail characteristics. The experimental data presented in this paper also provide the possibility of estimating the effect of a number of other factors, as for example, the form of the control surface leading edge.

The general method of computing the critical center-of-gravity location of the airplane (forward and backward) is considerably simplified. This is particularly true with reference to the critical backward center-of-gravity location for which the case of stick-free flight is the deciding one.

Of all three types of servo control considered (flap, cut-out, and outrigger), the most favorable from the point of view of application as balance tab is the cut-out type, since it is light and structurally simple to mount with the usual form of horizontal and vertical tail surfaces.

From the point of view of maximum "efficiency of balance" and minimum loss in effectiveness of the main-control surface, it is necessary to give the servo tab a larger aspect ratio.

By utilizing the "tip effect" in placing the servo tab outboard of the span a certain advantage can be gained, provided such a location does gives rise to possible vibration.

The servo tabs of the outrigger type for structural reasons cannot be conveniently mounted on the usual tail

surfaces. For those tail surfaces, however, for which a very large control-surface deflection is required, as for example, in the case of vertical surfaces of tailless airplanes, the outrigger type of servo tab will undoubtedly have the advantage over the other two types considered.

Servo controls are at the present time used essentially in the form of trimming tabs. The fact that servo-balance flaps notwithstanding their evident advantages over other types of balance in some cases give place to other means of balancing is in our opinion explained first by the fact that designers are improving the stability and controllability by a careful positioning of the center of gravity and by a careful choice of wing section and plan form. It is evident that by these means the problems of balancing and reduction of forces on the stick are simplified and at times make control-surface balance entirely unnecessary. In the second place, servo tabs, as has been shown in the present paper, tend to decrease the stability of an airplane with stick free and thirdly in the absence of weight balance of the control and with inaccurate design the critical speed at which vibrations are set up is lowered. A trimming tab does not have these defects of the servo-balance tabs and, with careful center-of-gravity location, may solve the problem.

There is a range, however, where servo-balance tabs are entirely feasible. This is true in the case of large-sized airplanes where servo motors of the electric and penumatic types, etc., are not used. As the size of the airplane is increased (up to a certain limit) the importance of servo-balance tabs increases and with full-weight balance of the control surface, they present one of the most suitable and effective means of reducing the stick forces. In this connection, systematic investigations of servo-balance tabs on airplanes should be undertaken, since there are practically no data available.

Translation by S. Reiss,
National Advisory Committee
for Aeronautics.

REFERENCES

1. Bréguet, Louis: Stabilité longitudinale des avions. Révue General de l'Aéronautique, No. 6, 1925.

Goroshenko: Longitudinal Stability of an Airplane. Technika Vosdushnogo Flota, Nos. 7-8, 1929.

Jouravchenko, A. N., & Nikitiuk, A. I.: On the Measurement of the Statical Longitudinal Stability of Airplanes. CAHI Report No. 94, 1931.

2. Glauert, H.: Theoretical Relationships for an Aerofoil with Hinged Flap. R. & M. No. 1095. British A.R.C., 1927.

3. Perring, W. G.A.: The Theoretical Relationships for an Aerofoil with a Multiply Hinged Flap System. R. & M. No. 1171. British A.R.C., 1928.

4. Ackeret, J.: Experiments on Airfoils with Trailing Edge Cut Away. T. M. No. 431, N.A.C.A., 1927.

5. Lotz, J.: Theorie von Flügeln mit Ausschnitten. Z.F.M., vol. 23, no. 14, July 28, 1932, pp. 410-413.

6. Okamoto, Tetusi: The Experimental Investigation on the Effects of a Cut-Out on the Wing Characteristics (Pt. I). Aeronautical Research Institute, Tokyo Imperial University, vol. 9, no. 5, October 1934, pp. 103-137. Report No. 113.

7. Biechteler, Curt. Influence of Cut-Outs in Elevator on the Static Longitudinal Stability and on the Static Elevator Effect. T. M. No. 750, N.A.C.A., 1934.

8. Kolosov, E.: Investigation of Tail Surfaces with Servo Controls. Technical Note No. 55, CAHI, 1935.

9. Reid, Elliott G.: Servo-Control Flaps. Jour., Aero. Sci., October 1934, pp. 155-167.

10. Stack, John, & von Doenhoff, Albert E.: Tests of 16 Related Airfoils at High Speeds. T. R. No. 492, N.A.C.A., 1934.

11. Targue, C. M.: Influence of the Wing on the Static Longitudinal Stability of the Airplane. Technika Vosdushnogo Flota No. 9, 1933.

12. Goncharov, B. F.: Selection of Control Members for an Airplane. Technical Note No. 34, CAHI, 1934.

TABLE I

Tail surface	1	1a	2	2a	2b	3	3a	4	4a	5	6	7	7a	8	9	9-1
Thickness ratio, σ in %	8	8	8	8	8	8	8	8	8	8	9	8	8	12	12	12
$\lambda = \frac{l^2}{S_{true}}$	3	3.08	3	3.08	3.25	3	3.08	3	3.08	3	3.5	3	3	3.5	3.5	3.5
$\frac{S_{ca.}}{S_t}$ %	39.5	37.7	39.4	37.5	34.1	39.8	38	40.3	38.1	39.7	44.6	60	60	60	50	50
$\frac{S_{bal}}{S_{ca.}}$ %	17.7	19.1	17.6	19.13	22.2	17.55	18.95	18.33	20	17.5	14.1	15.34	15.34	0	0	20
$\frac{S_{cut-out}}{S_{ca.}}$ %	0	8.0	0	8.6	26	0	8	0	9	0	6	0	0	0	0	0
$\frac{S_{with\ cut-out}}{S_{tail\ surf.with\ cut-out}}$ %	0	3.0	0	3	8.8	0	3	0	3	0	2.6	0	0	0	0	0
Wind tunnel data																
$\frac{\partial c_y}{\partial \alpha}$ at $\delta = 0^\circ$	.0261	.02675	.0287	.0269	.0269	.0271	.0263	.026	.0274	.0294	-	.0265	.0262	-	.0255	.0255
$\frac{\partial c_y}{\partial \delta}$ at $\alpha = 0^\circ$	.0146	.0134	.0143	.0154	.0117	.0185	.0135	.0153	.0137	.0157	.015 .0165	.026	.03175	.021	.0196	.0198
Hinge-moment coefficient based on mean geometric chord of control surface																
$\frac{\partial c_h}{\partial \alpha}$ at $\delta = 0^\circ$	.000425	.000545	.00094	.00043	.00016	.0004	.0007	.0005	.0004	.0008	.00102	.0017	.0013	-	-	.0009
$\frac{\partial c_h}{\partial \delta}$ at $\alpha = 0^\circ$	.00252	.00218	.00309	.00237	.00209	.0025	.0024	.00235	.00182	.00255	.0024 .00352	.00344	.00267	.0049	.00545	.00178
Hinge-moment coefficient based on maximum chord of control surface																
$\frac{\partial c_h}{\partial \alpha}$ at $\delta = 0^\circ$	.0003	.0004	.0007	.0003	.0001	.0004	.0007	.0005	.0004	.0008	.0009	.0017	.0013	-	-	.0009
$\frac{\partial c_h}{\partial \delta}$ at $\alpha = 0^\circ$	.00178	.0015	.0023	.00165	.0013	.0025	.0024	.00235	.00182	.0255	.00212 .00311	.00344	.00267	.0049	.00545	.00178
Computed data																
$\frac{\partial c_y}{\partial \delta}$ at $\alpha = 0^\circ$	.01467	.0134	.01467	.0133	.1083	.01472	.01347	.01473	.01325	.01472	.0162	.01845	.01845	.022	.02	.017

Tail surface	10	11	11a	12	13	13a	13b	13c	14	16	16-1	16-2	16-3	15	17	18
Thickness ratio, σ in %	12	8	8	8	8	8	8	8	10.5	6	6	6	6	-	-	-
$\lambda = \frac{l^2}{S_{true}}$	3.5	3.81	4.25	4.1	3.74	3.99	4.12	4.27	4.75	4.04	4.04	4.04	4.04	4.83	4.53	5.53
$\frac{S_{ca.}}{S_t}$ %	40	59	54.6	62	65.1	62.8	61.6	60.2	41.3	45	45	45	45	33	38.7	38.3
$\frac{S_{bal}}{S_{ca.}}$ %	0	3	3	6.95	6	6.65	7.03	7.43	3	0	10.6	16.8	22.8	28	28	25
$\frac{S_{cut-out}}{S_{ca.}}$ %	0	0	20	16.5	0	10.73	16.75	23	11.3	10.6	10.6	10.6	10.6	6	6	6
$\frac{S_{with\ cut-out}}{S_{tail\ surf.with\ cut-out}}$ %	0	0	10.85	10.2	0	6.75	10.32	14.15	4.7	4.8	4.8	4.8	4.8	2	2	2
Wind tunnel data																
$\frac{\partial c_y}{\partial \alpha}$ at $\delta = 0^\circ$	-	.0307	.0276	.02845	.0285	.0287	.029	.0291	.029	.0304	.0295	.029	.0304	-	-	-
$\frac{\partial c_y}{\partial \delta}$ at $\alpha = 0^\circ$	.017	.0229	.0183	.0193	.0225	.022 .021	.01925 .02	.0185 .0192	.017	.0196	.0177	.017	.0155	-	-	-
Hinge-moment coefficient based on mean geometric chord of control surface																
$\frac{\partial c_h}{\partial \alpha}$ at $\delta = 0^\circ$	-	.00306	.00331	.00272	.0037	.00355	.00347	.00333	.0019	.00354	.00271	.00177	.00118	.00028	.000505	.00028
$\frac{\partial c_h}{\partial \delta}$ at $\alpha = 0^\circ$	.0053	.00187	.00413	.00355	.00527	.00534	.00511	.00417	.00405	.00688	.00372	.00377	.001663	-	-	-
Hinge-moment coefficient based on maximum chord of control surface																
$\frac{\partial c_h}{\partial \alpha}$ at $\delta = 0^\circ$	-	.0022	.00198	.0021	.0033	.00286	.00255	.0024	.00138	.003	.0023	.0015	.001	.00022	.00046	.00024
$\frac{\partial c_h}{\partial \delta}$ at $\alpha = 0^\circ$	.0053	.0035	.00247	.00275	.0047	.0043	.0039	.003	.00272	.00583	.00316	.00335	.00141	-	-	-
Computed data																
$\frac{\partial c_y}{\partial \delta}$ at $\alpha = 0^\circ$	.018	.0219	.01847	.01955	.0223	.0205	.01945	.0183	.01788	.0183	.01884	.016	.01517	-	-	-

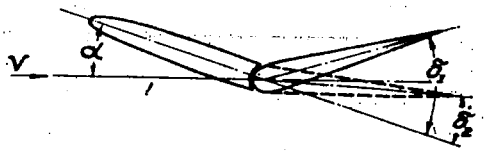

Figure 1

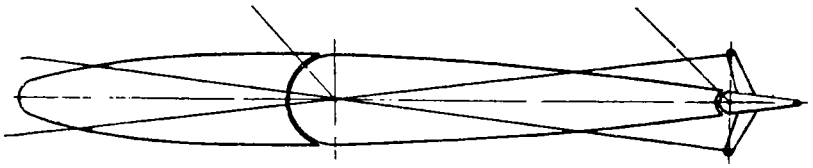

Figure 2.- Sketch of servo control device.

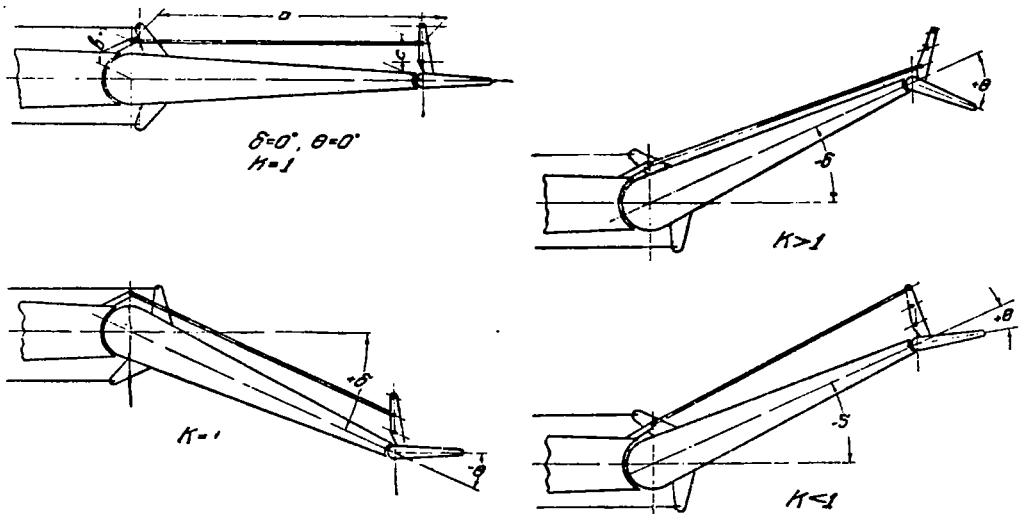

Figure 3.- Control with servo balance tab.

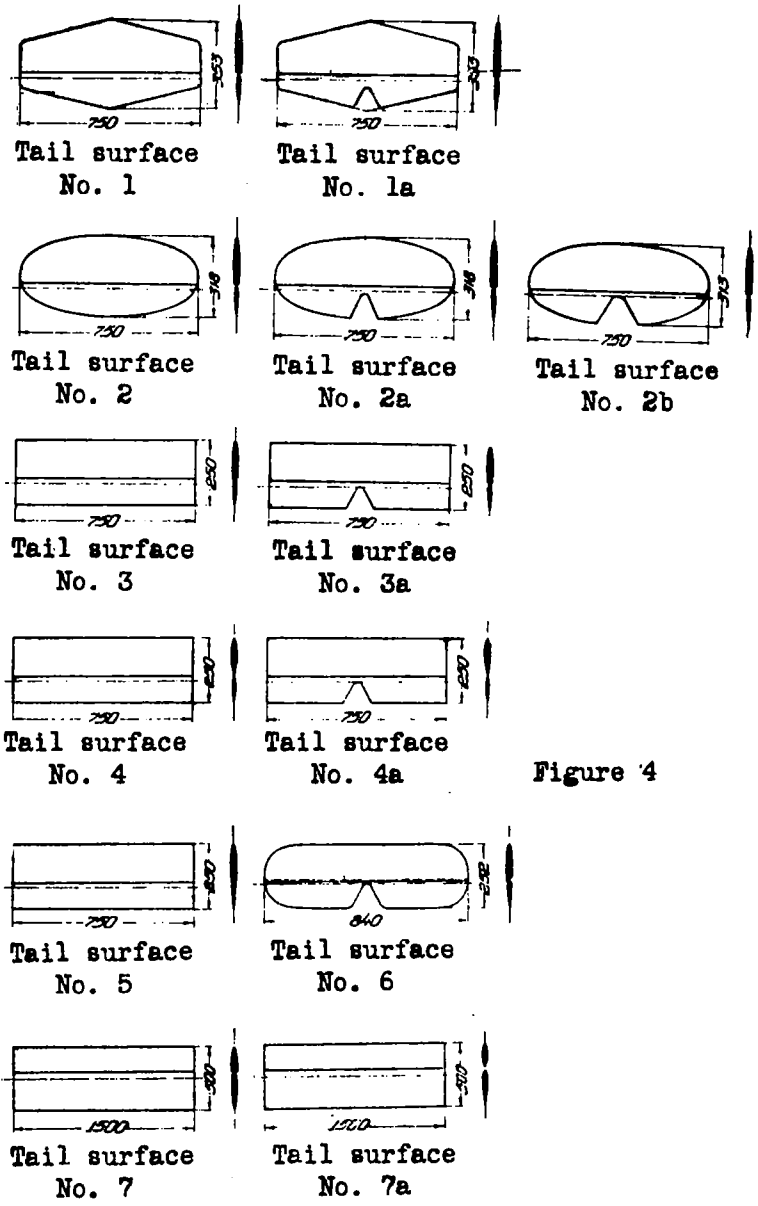

Figure 4

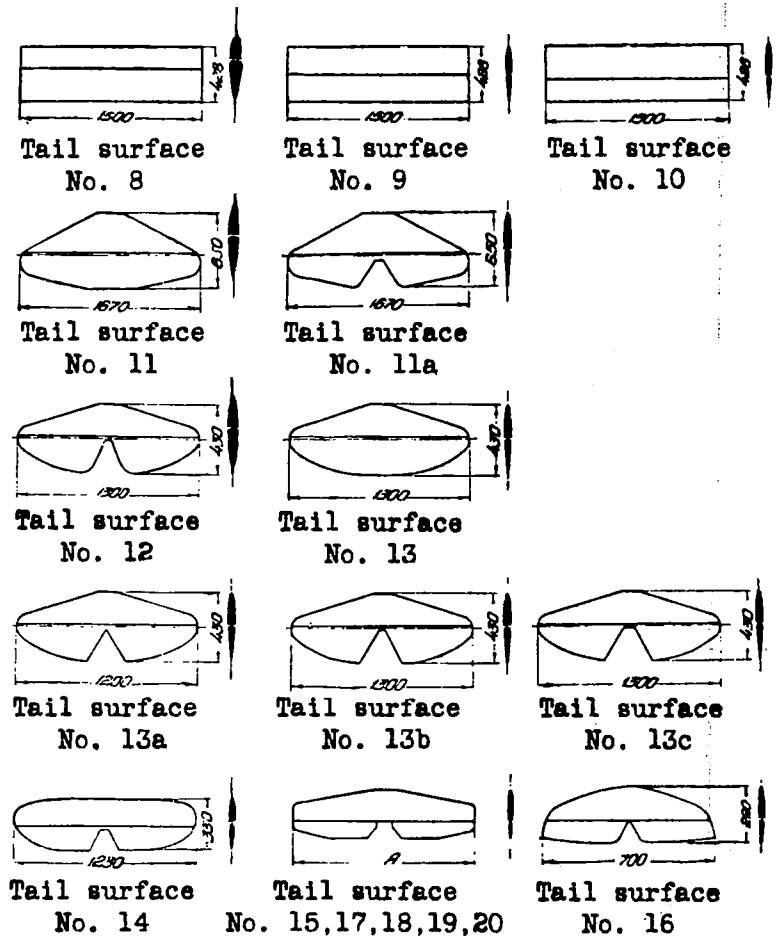

Figure 4a.- Sketch of tail surfaces tested.

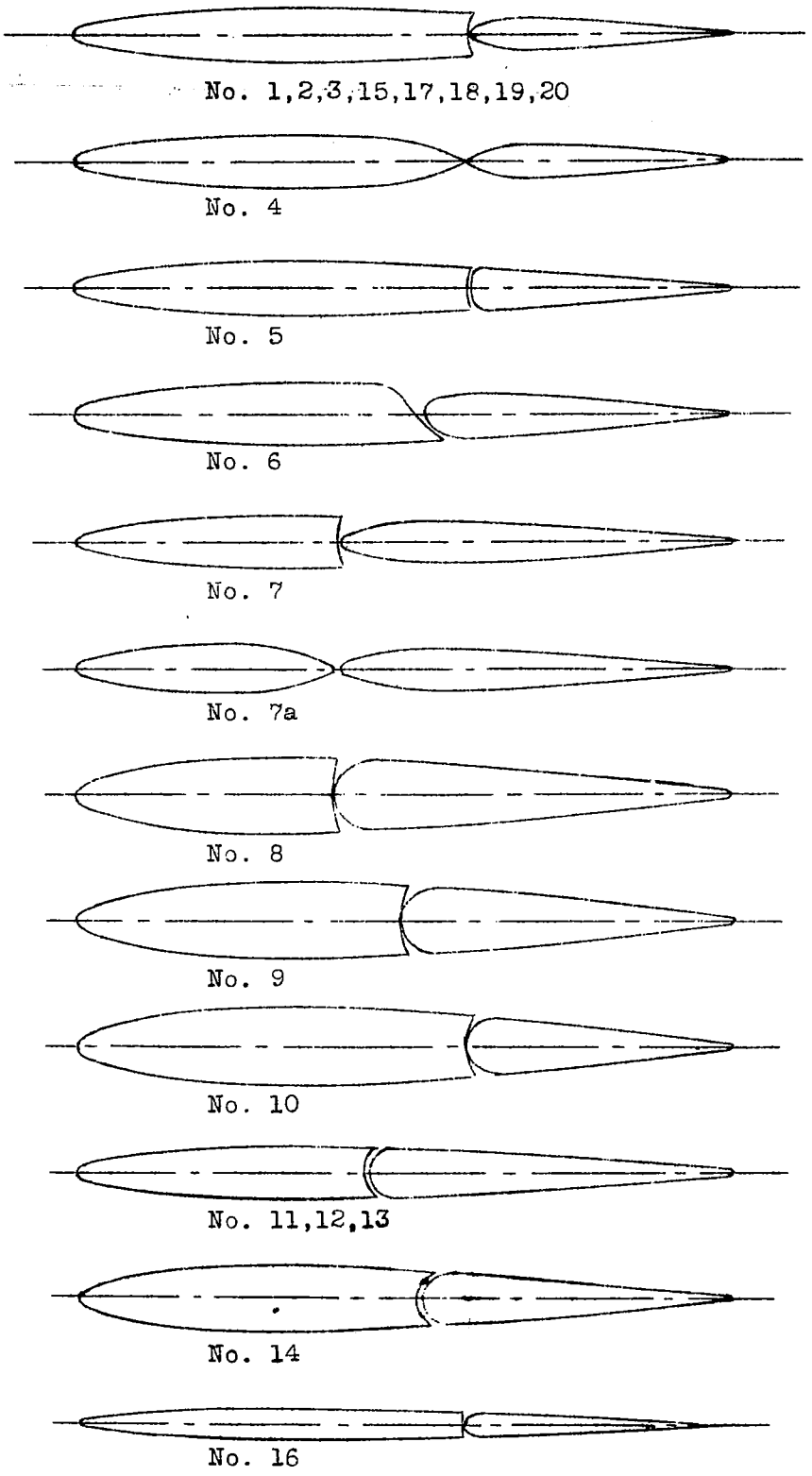

Figure 4b.- Profiles of tail surfaces tested.

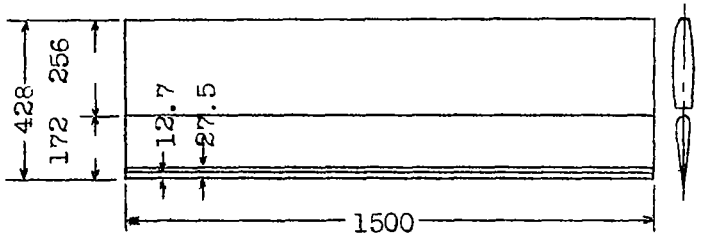

Tail surface No. 8

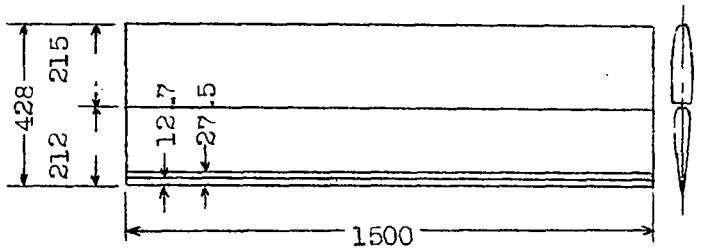

Tail surface No. 9

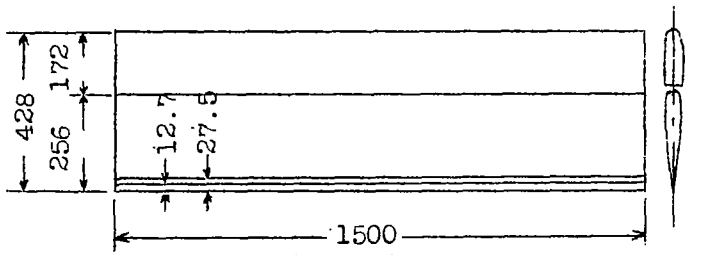

Tail surface No. 10

Figure 5.- Tail surface with flap type of servo control tab.

Without cut-out ——————

With cut-out —————— at full throttle.
- - - - - - - with power off.

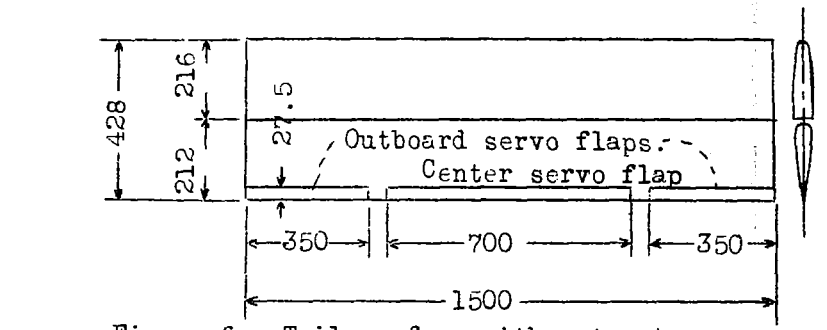

Figure 6.- Tail surface with cut-out servo control tab.

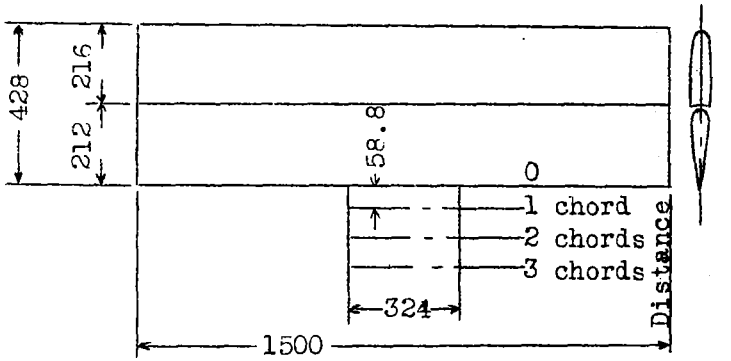

Figure 7.- Tail surface with outrigger type servo control tab.

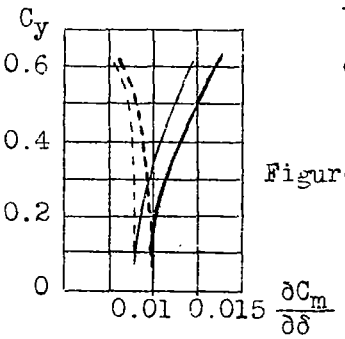

Figure 12.- $\frac{\partial C_m}{\partial \delta}$ as a function of C_y (according to flight tests by Bichtler).

Figs 5,6,7,12

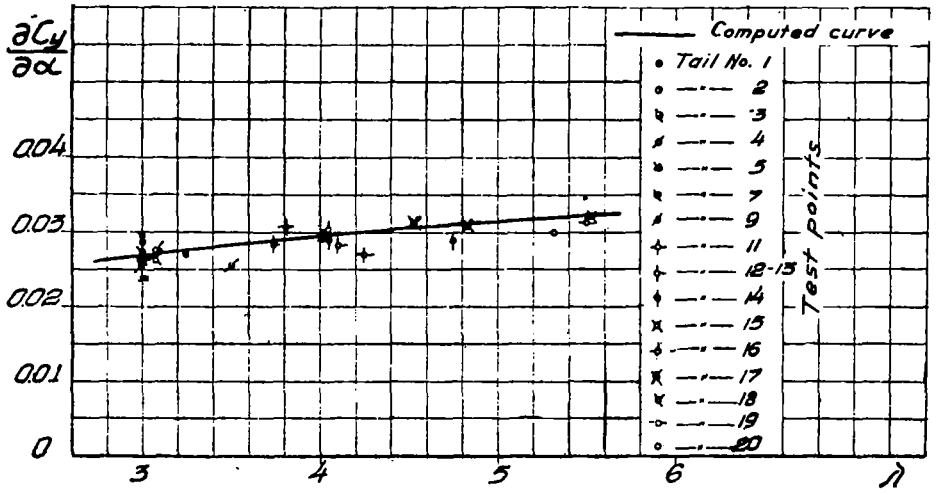

Figure 8.- Lift coefficient slope as computed by formula and as obtained in tests.

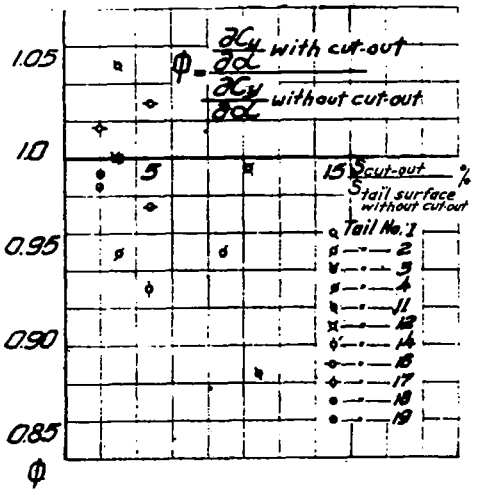

Figure 9.- Variation of $\frac{\partial C_y}{\partial \alpha}$ with change in cut-out area.

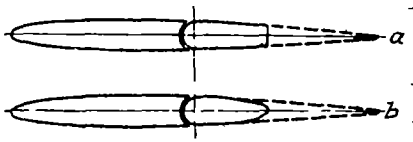

Figure 10.- Forms of trailing edge of control surface after cut-out.

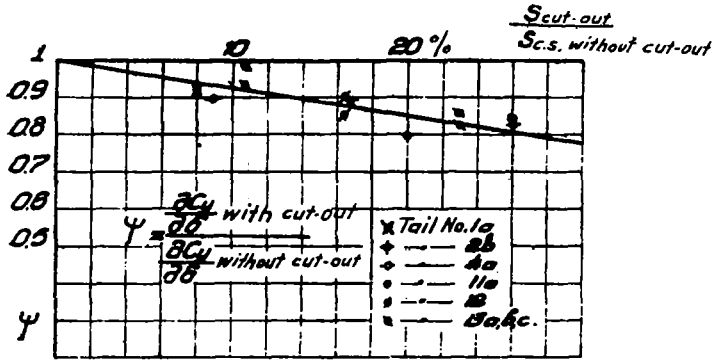

Figure 11.- Variation of $\frac{\partial C_y}{\partial \delta}$ with change in cut-out area.

Figure 13.- Test curves of C_y against $f(\delta_p)$ for tail No. 9 with 6 percent servo-area and 20 percent balance.

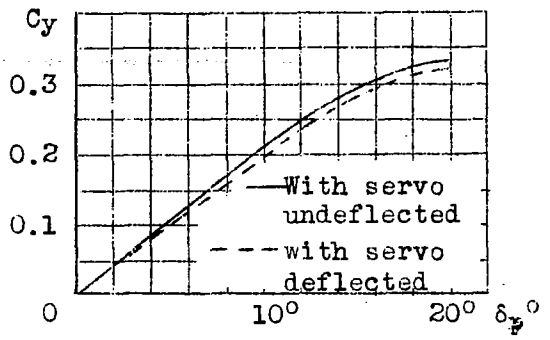

Figure 14.- Curves of control surface lift coefficient C_y with 5 percent servo of the flap type.

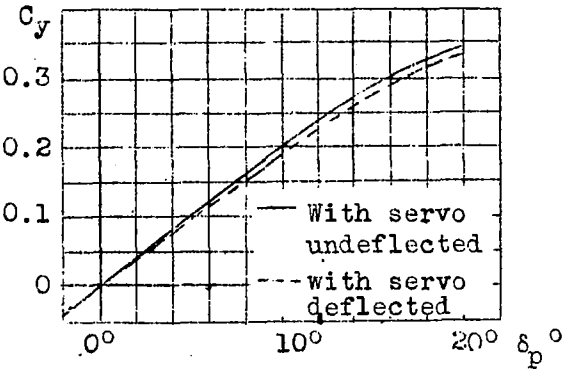

Figure 15.- Curves of control surface lift coefficients C_y with 6 percent servo of the flap type.

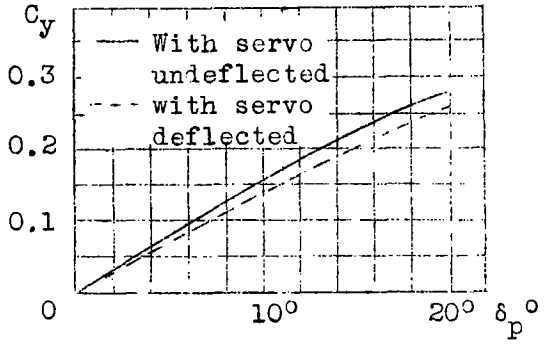

Figure 16.- Curves of control surface lift coefficients C_y with 7.5 percent of the flap type.

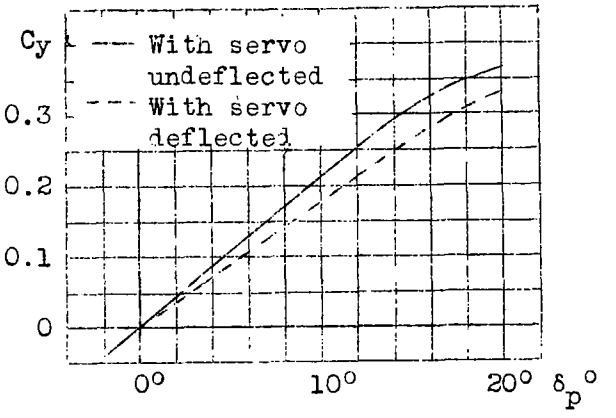

Figure 17.- Curves of control surface lift coefficients C_y with 10.75 percent servo of the flap type.

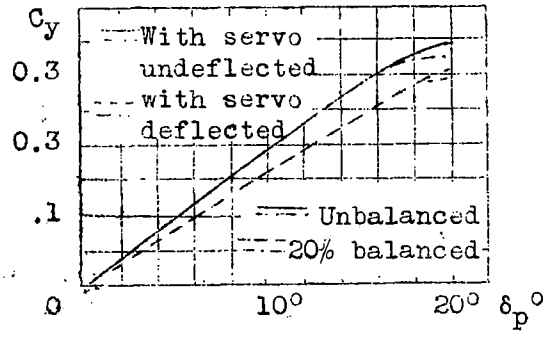

Figure 18.- Curves of lift coefficients of control surface with 13 percent servo of the flap type.

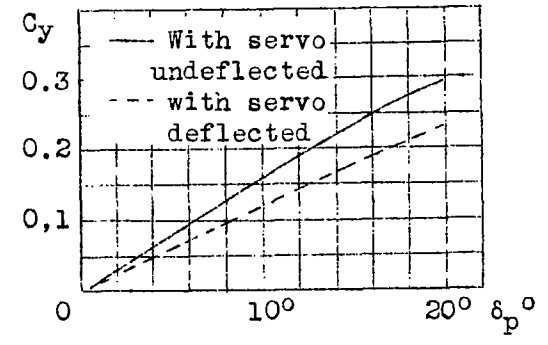

Figure 19.- Curves of lift coefficients of control surface with 16 percent servo of the flap type.

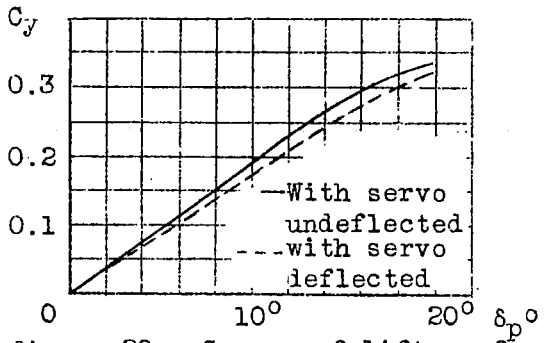

Figure 20.- Curves of lift coefficients of control surface with 6 percent servo of the cut-out type.(center flap).

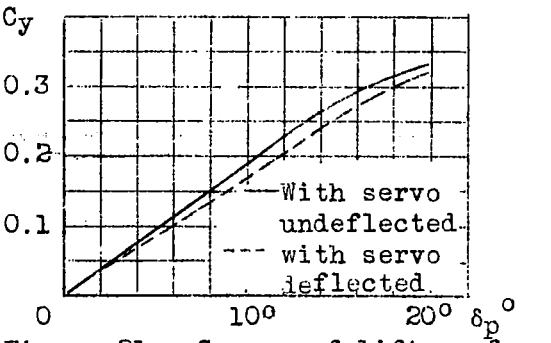

Figure 21.- Curves of lift coefficients of control surface with 6 percent servo of the cut-out type (outboard flaps)

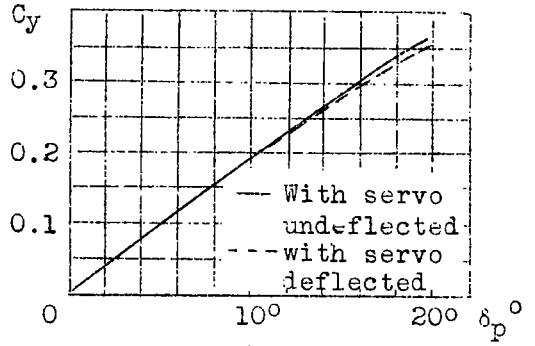

Figure 22.- Curves of lift coefficients of control surface with 6 percent outrigger tab. Outrigger distance 3 chords.

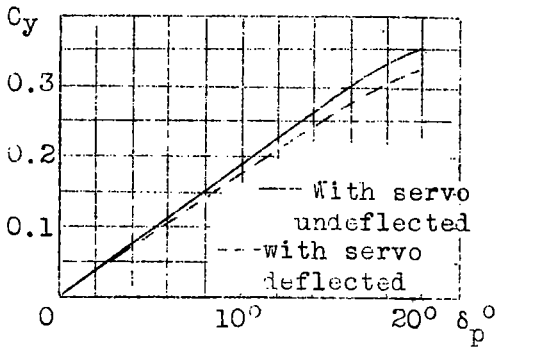

Figure 23.- Curves of lift coefficients of control surface with 6 percent outrigger tab. Outrigger distance zero.

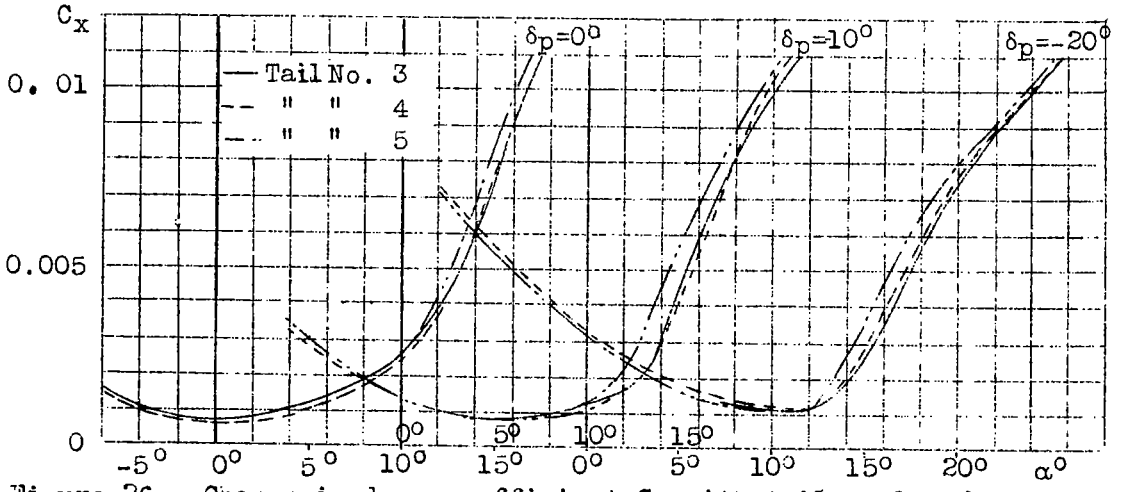

Figure 26.- Change in drag coefficient C_x with tail angle of attack α for various settings of the control surface and for various forms of the control surface leading edge.

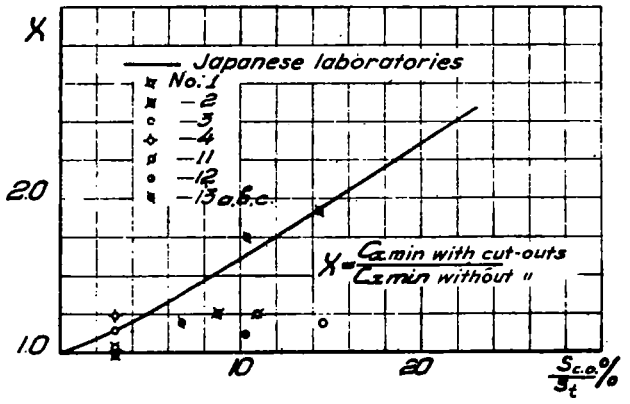

Figure 24.- Change of $C_{x_{min}}$ with change in cut-out area.

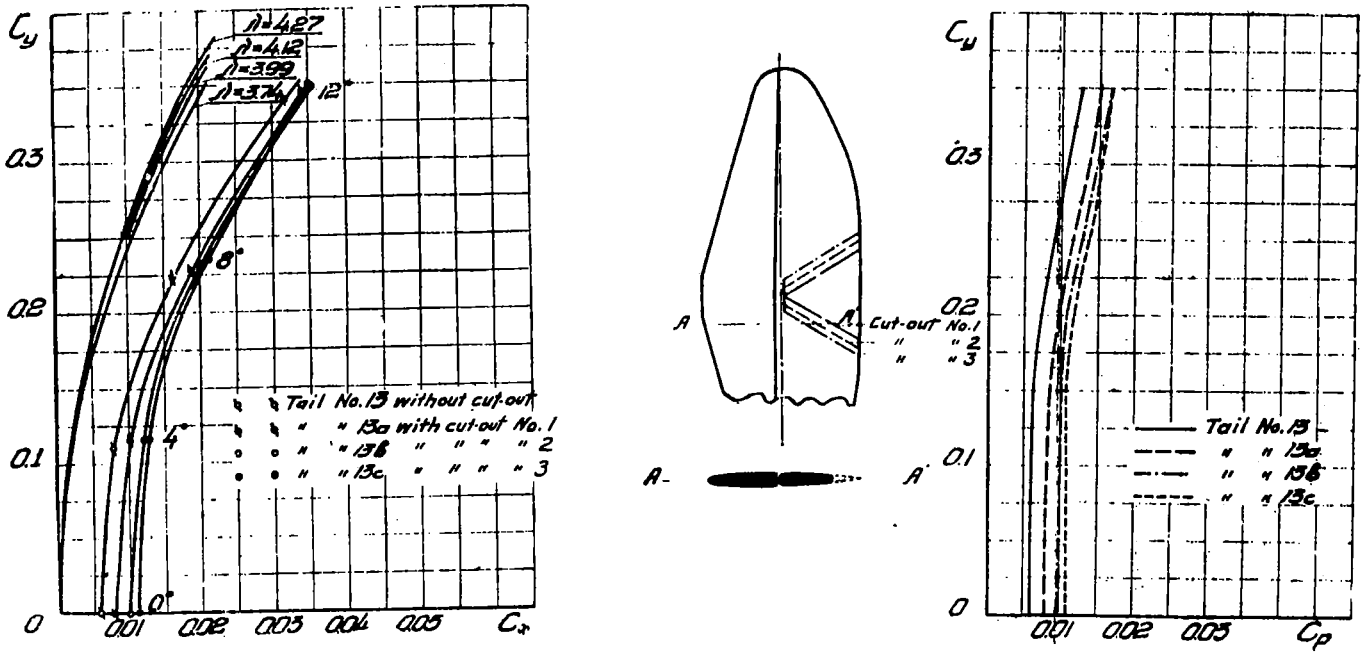

Figure 25.- Polar curves of model tail surface with various cut-outs for tail surface No. 13. The polars were drawn from test data.

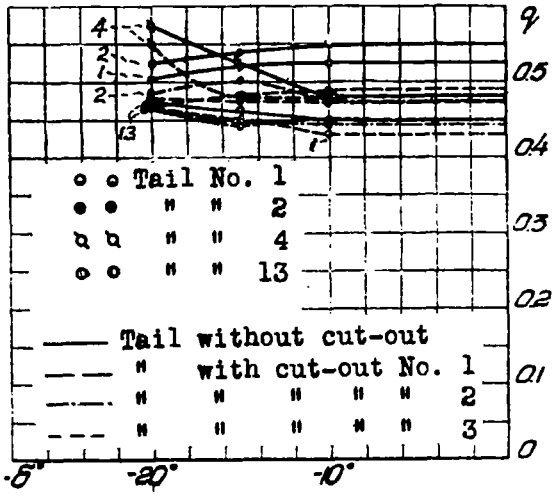

Figure 27.- Change in $q_\delta \frac{\partial C_m}{\partial C_y}$ with deflection of control surface.

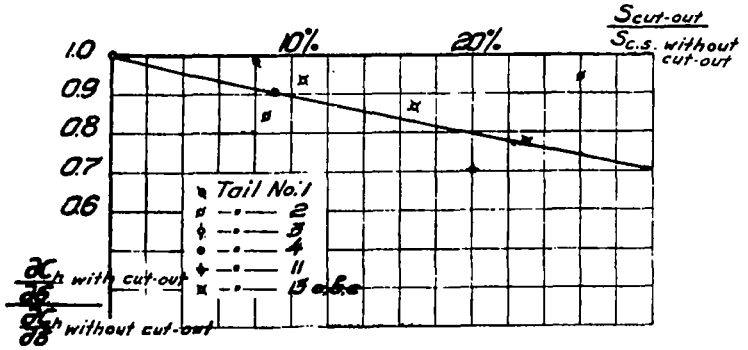

Figure 30.- Change in $\frac{\partial C_h}{\partial \delta}$ with cut-out area.

Figure 28.

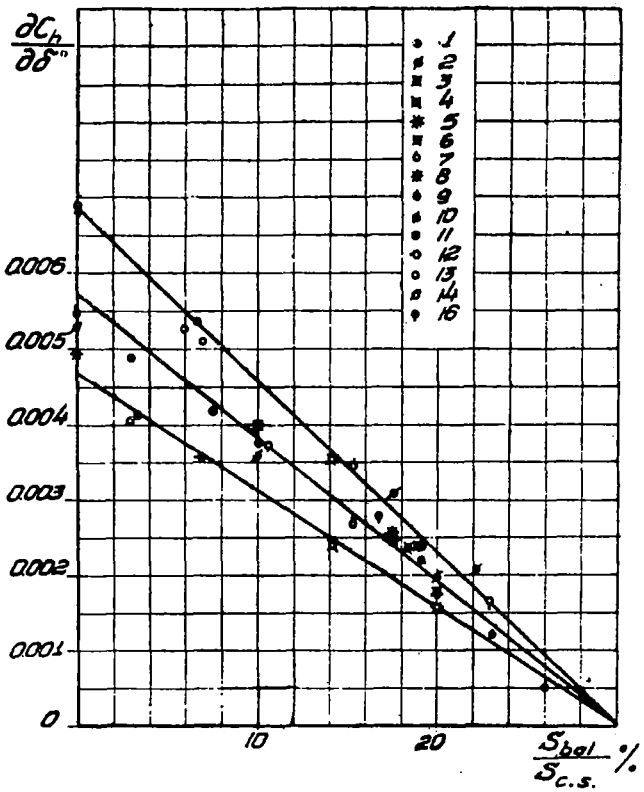

Figure 29.- $\frac{\partial C_h}{\partial \delta}$ plotted as a function of $\frac{S_{bal}}{S_{c.s.}}$ (the values are referred to the mean geometric chord of the control surface).

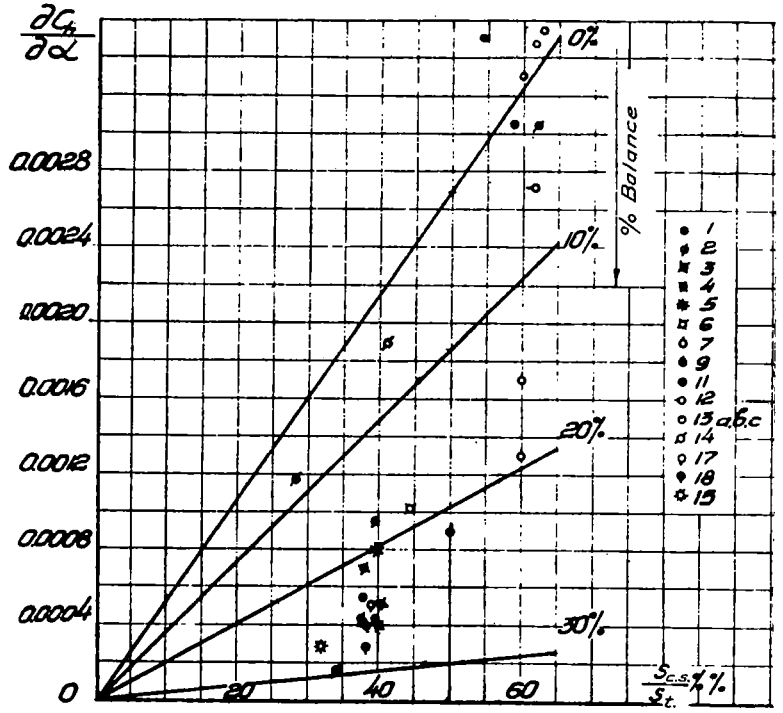

Figure 31.- Plot of $\frac{\partial C_h}{\partial \alpha}$ as a function of $\frac{S_{c.s.}}{S_t}$ and $\frac{S_{bal}}{S_{c.s.}}$ referred to mean geometric chord of control surface.

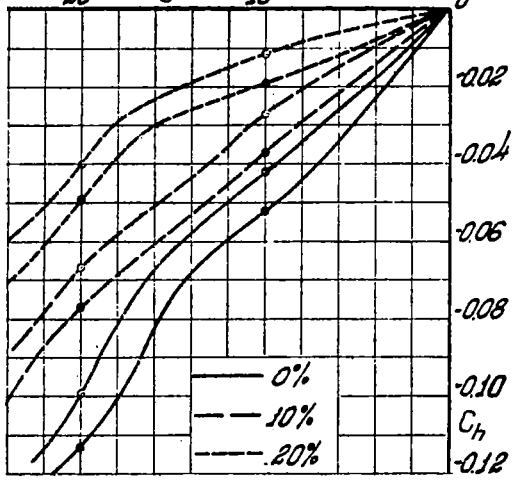

Figure 33.- Curves of hinge moments with 5% servo and various percent balance.

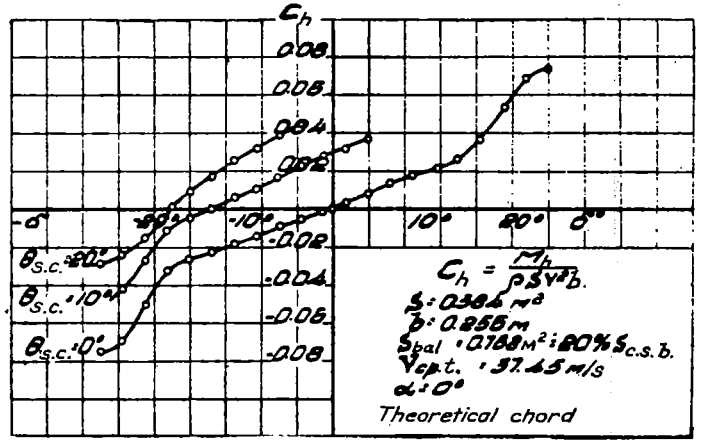

Figure 32.-Results of tests on elevator hinge moment with 10.75% servo.

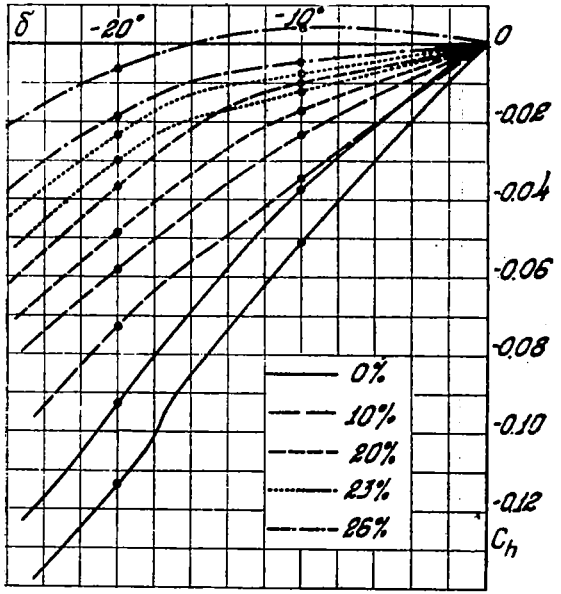

Figure 34.- Curves of hinge moments with 6% servo and various percent balance.

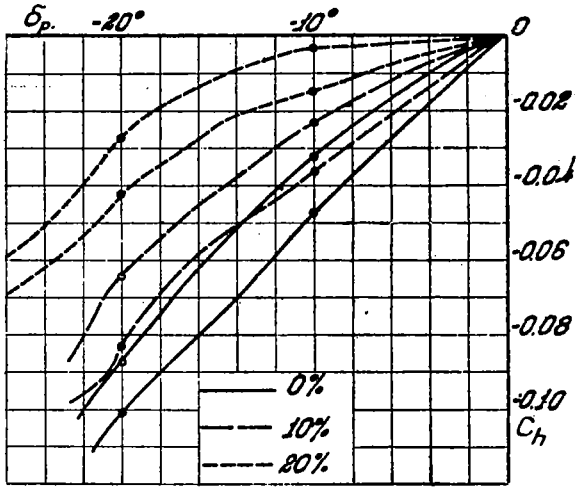

Figure 35.- Curves of hinge moments with 7.5% servo and various percent balance.

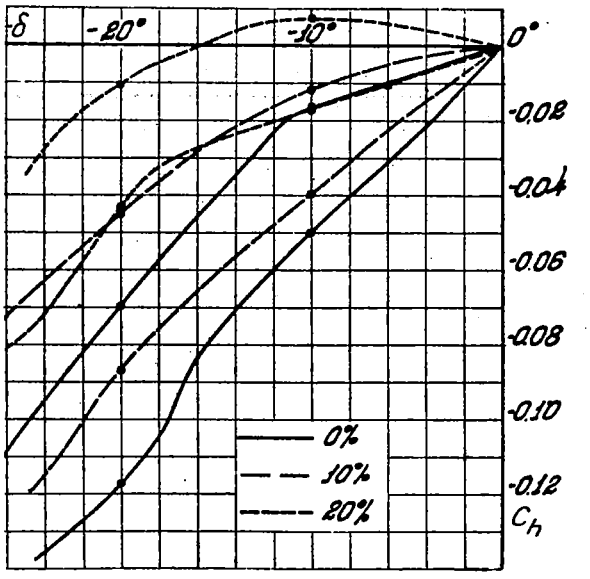

Figure 36.- Curves of hinge moments with 10.75% servo and various percent balance.

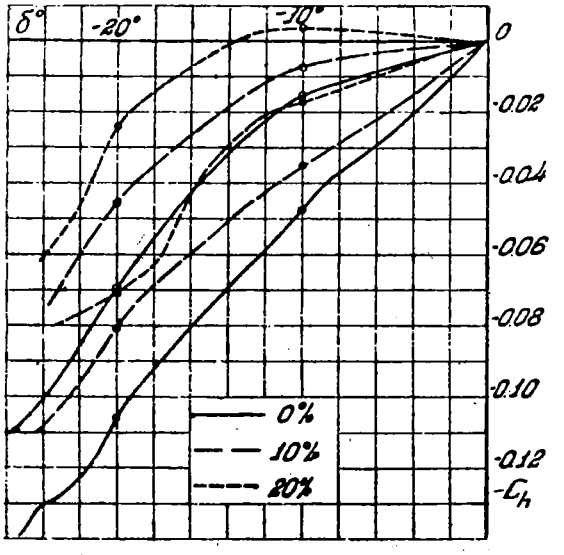

Figure 37.- Hinge moment curves with 13% servo and various percent balance.

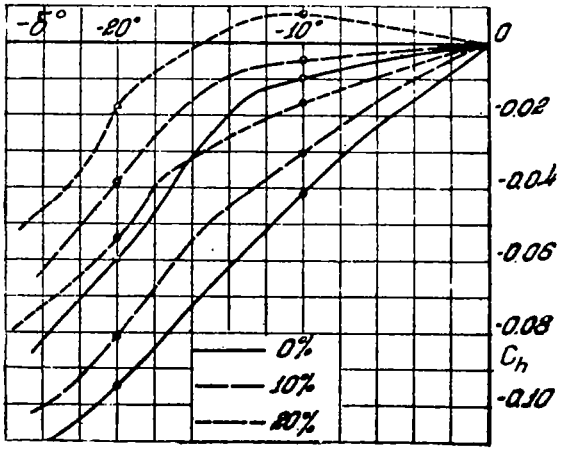

Figure 38.- Hinge moment curves with 16% servo and various percent balance.

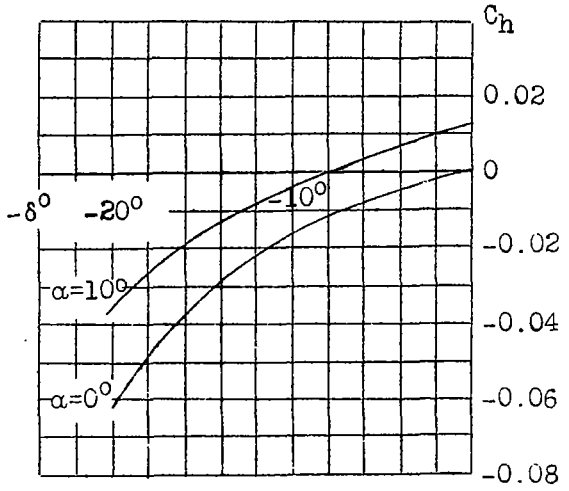

Figure 39.- Curves of C_h against δ for various stabilizer angles of attack α of tail surface No. 14 $S_{s.c.}$ = 6.44 percent of $S_{c.s.}$ for K= $\frac{\theta}{\delta}$ =1.

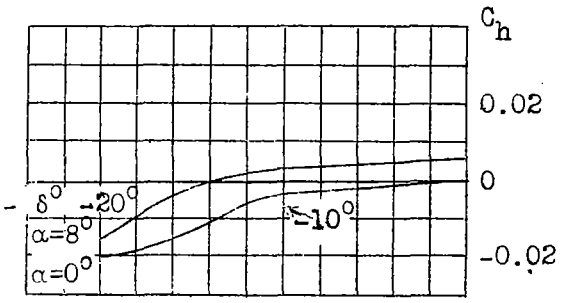

Figure 40.- Curves of hinge moment coefficients C_h against control surface deflection δ for various stabilizer angles of attack α, tail surface No. 11. $S_{s.c.}$ = 10 percent of $S_{cont.surf.}$ for K= $\frac{\theta}{\delta}$ =1.

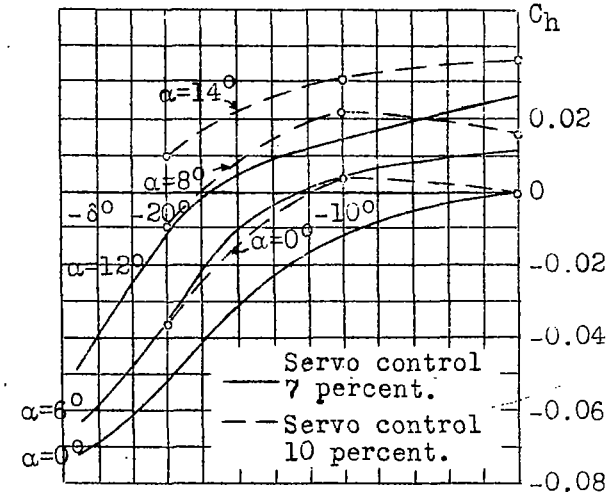

Figure 41.- Curves of C_h against δ for various angles of attack α of tail surface No. 12 with 7 and 10 percent servo control for K= $\frac{\theta}{\delta}$ =1.

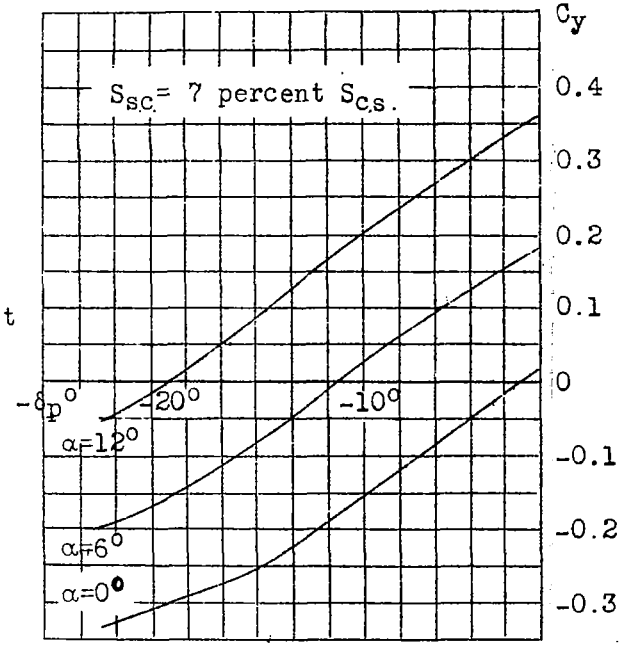

Figure 42.- Curves of C_y against δ for various angles of attack of the stabilizer, tail surface No. 12 with servo tab for K= $\frac{\theta}{\delta}$ =1.

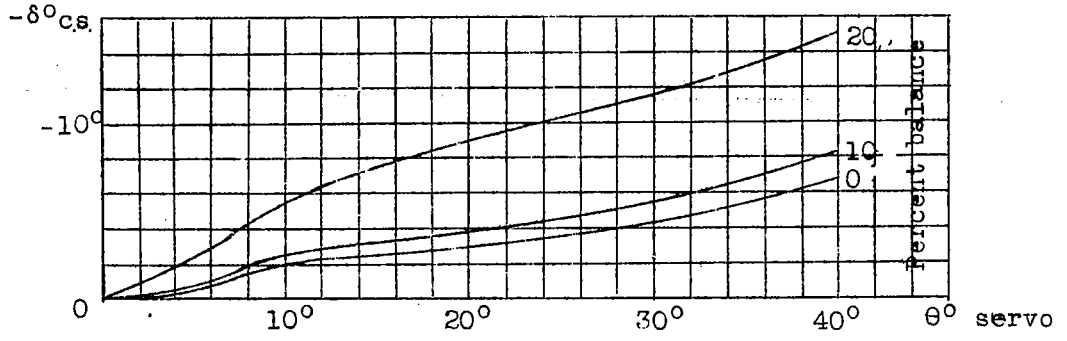

Figure 43.- Curves of equilibrium angles with 5 percent servo of flap type and with various percent axial balance.

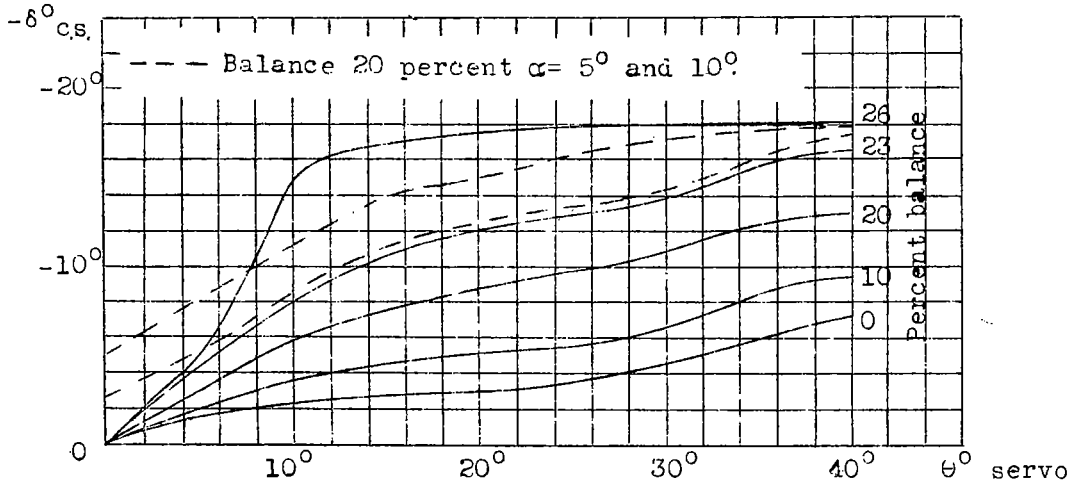

Figure 44.- Curves of equilibrium angles with 6 percent servo of flap type and various percent balance.

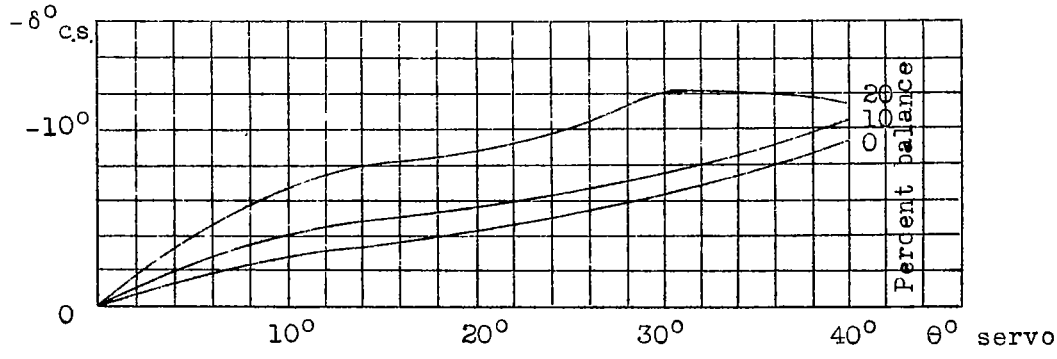

Figure 45.- Curves of equilibrium angles with 7.5 percent servo of flap type and various percent balance.

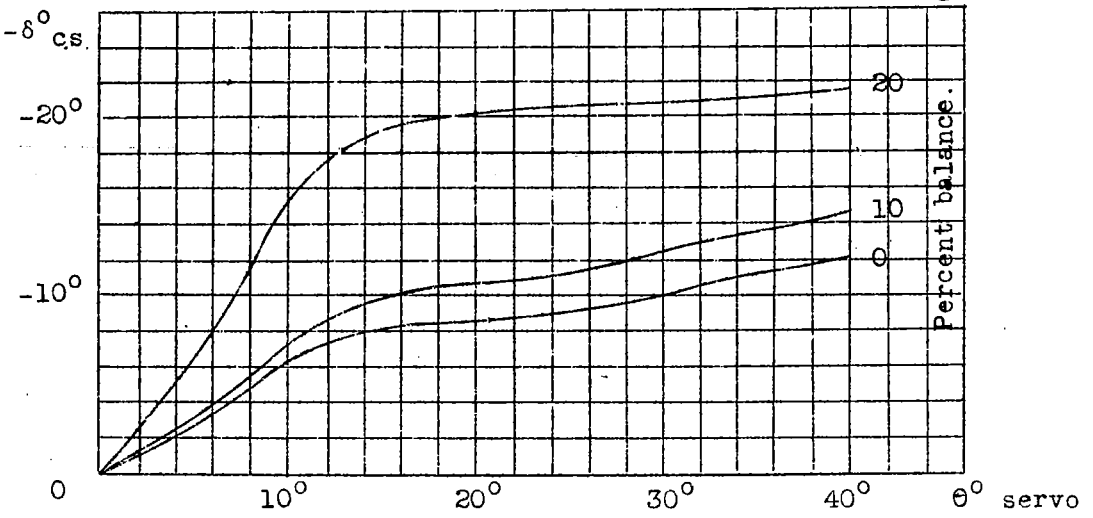

Figure 46.- Curves of equilibrium angles with 10.75 percent servo of the flap type and various percent balance.

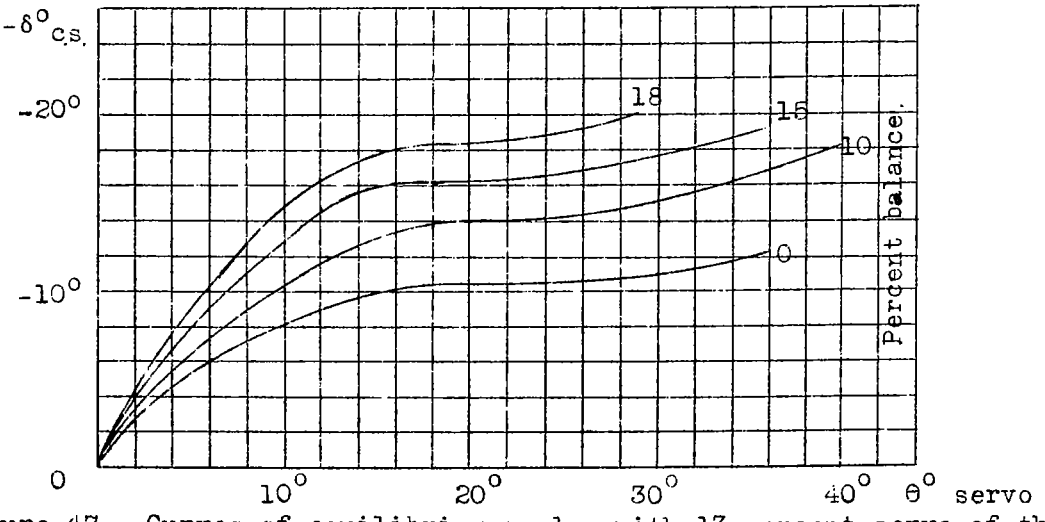

Figure 47.- Curves of equilibrium angles with 13 percent servo of the flap type and various percent balance.

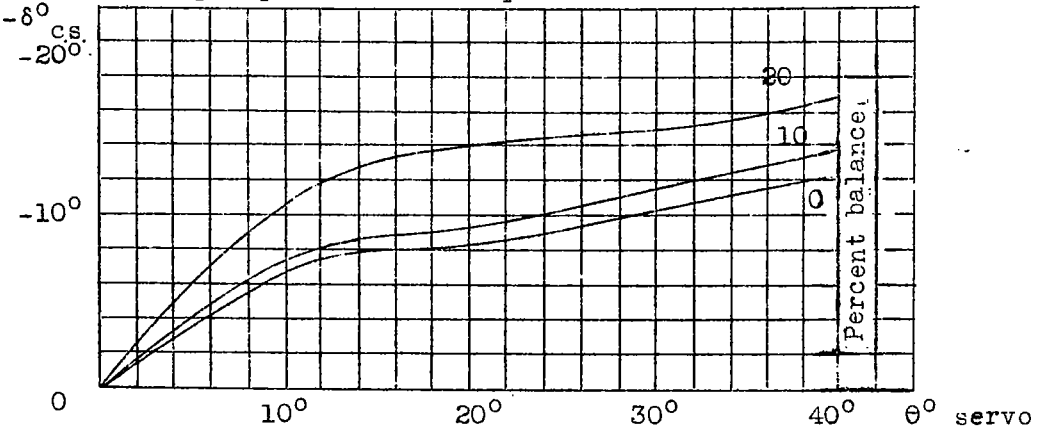

Figure 48.- Curves of equilibrium angles with 16 percent servo control of the flap type and various percent balance.

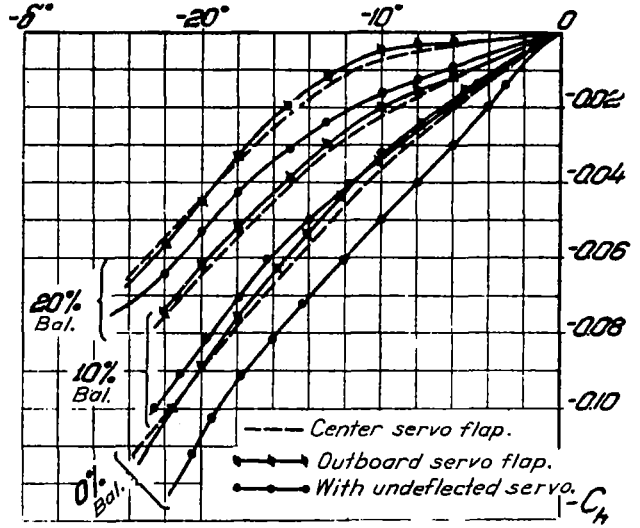

Figure 49.- Hinge moment curves with cut-out servo tabs and various percent balance.

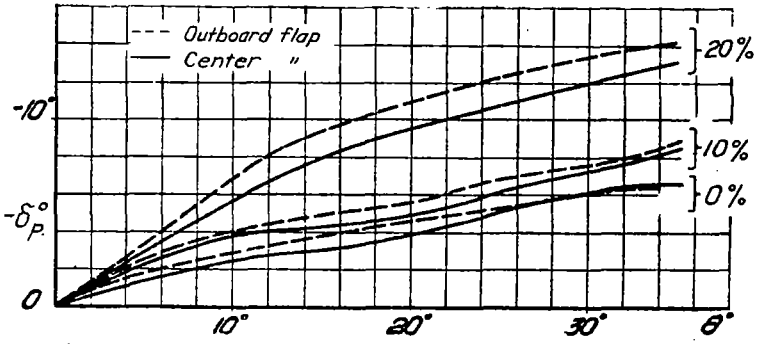

Figure 50.- Curves of equilibrium angles with 6% servo and various percent balance.

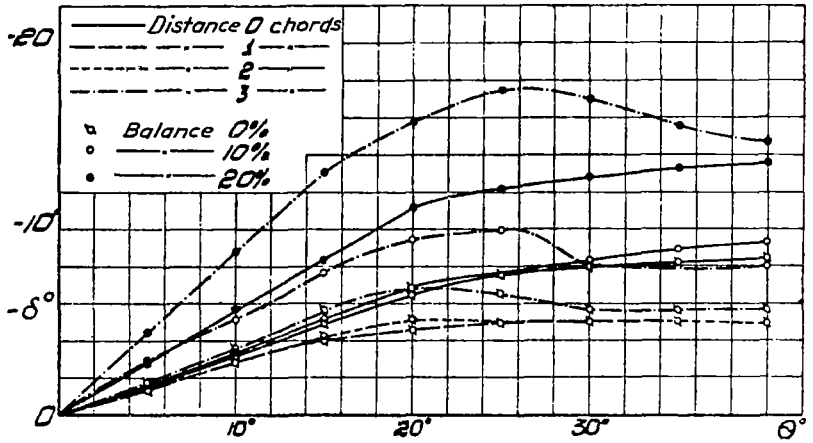

Figure 52.- Curves of equilibrium angles with 6% servo tab of outrigger type at various distances from trailing edge and with various percent balance.

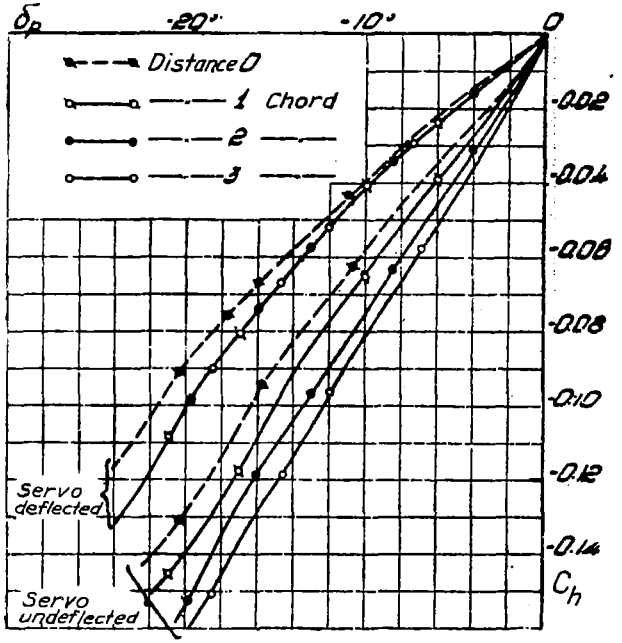

Figure 51.- Hinge moment curves with 6% servo tab of outrigger type at various distances from trailing edge.

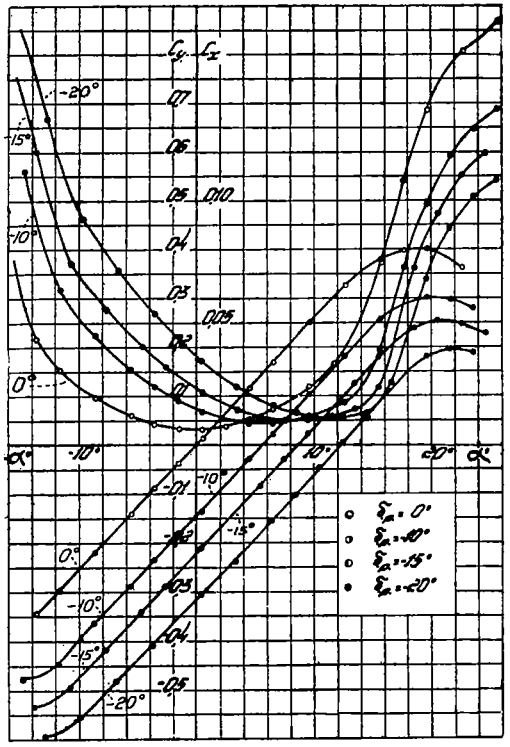

Figure 53.- Tail surface No. 1.

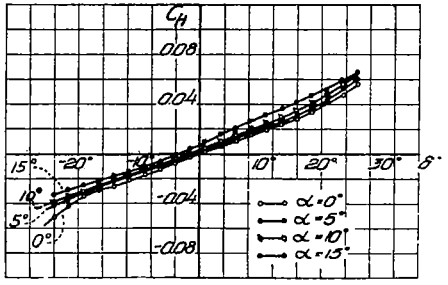

Figure 54.- Tail surface No. 1.

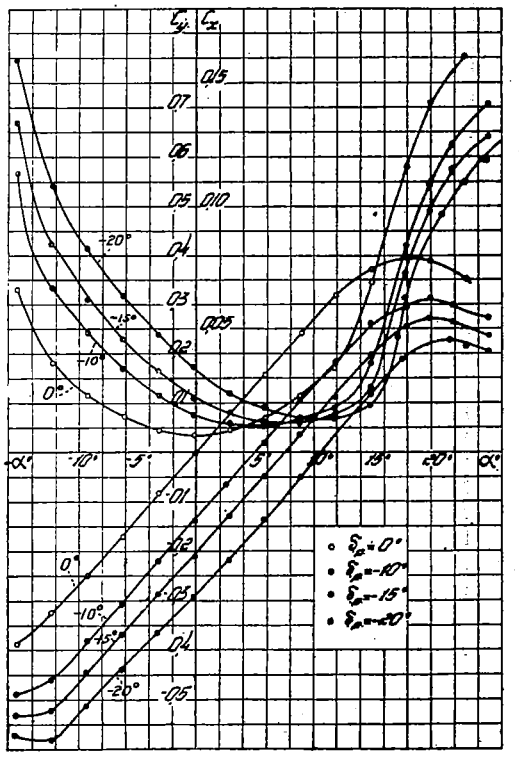

Figure 55.- Tail surface No. 1a.

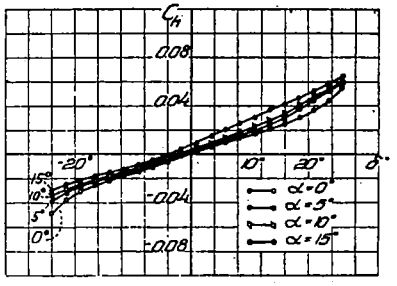

Figure 56.- Tail surface No. 1a.

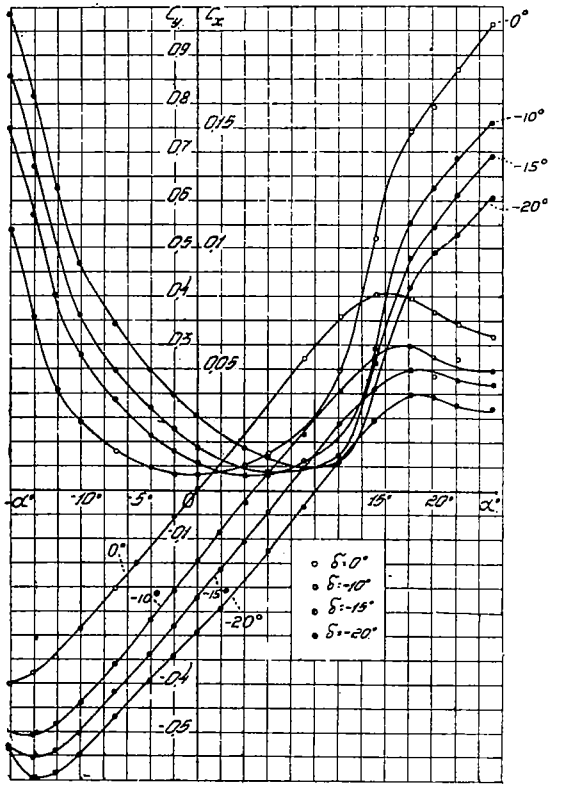

Figure 57.- Tail surface No. 2.

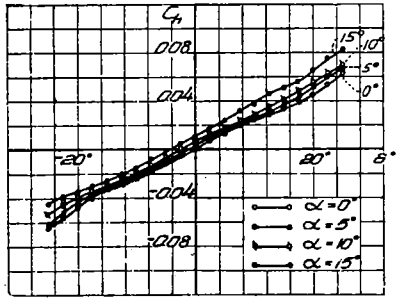

Figure 58.- Tail surface No. 2.

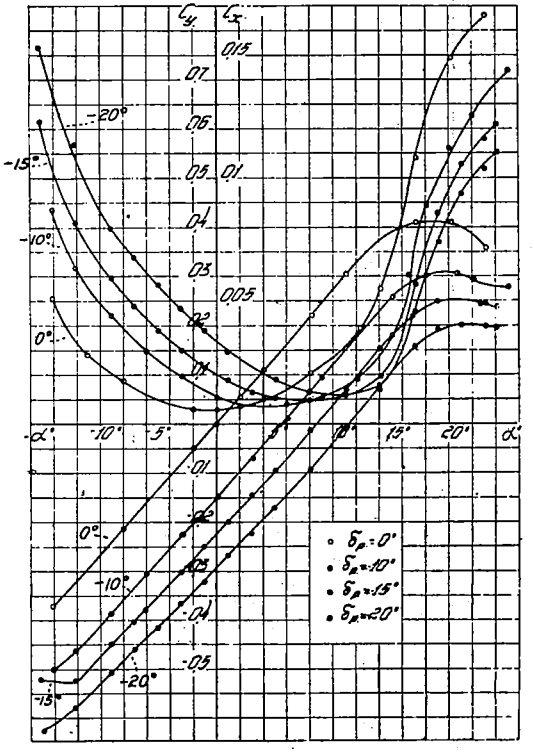

Figure 59.- Tail surface No. 2a.

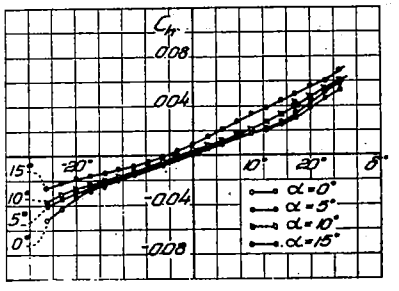

Figure 60.- Tail surface No. 2a.

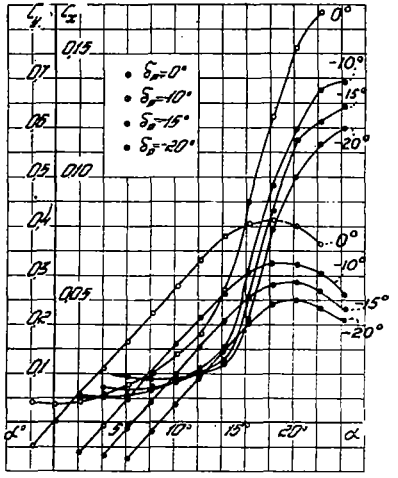

Figure 61.- Tail surface No. 2b.

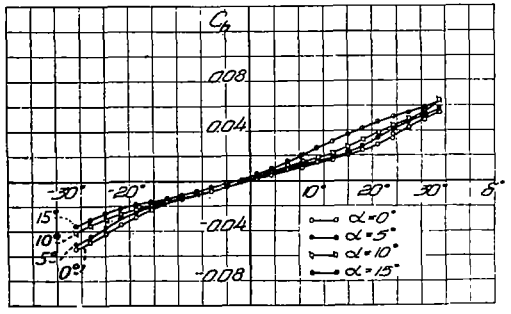

Figure 62.- Tail surface No. 2b.

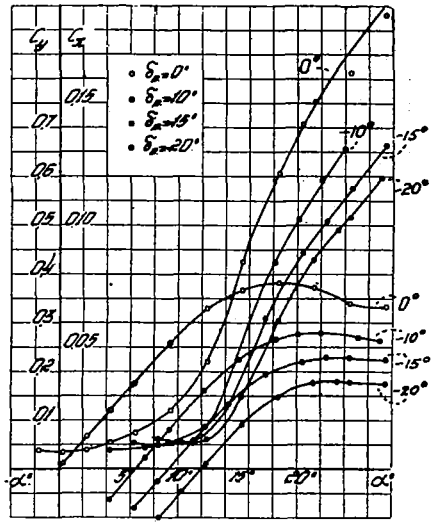

Figure 63.- Tail surface No. 3.

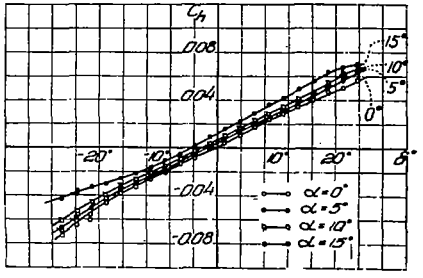

Figure 64.- Tail surface No. 3.

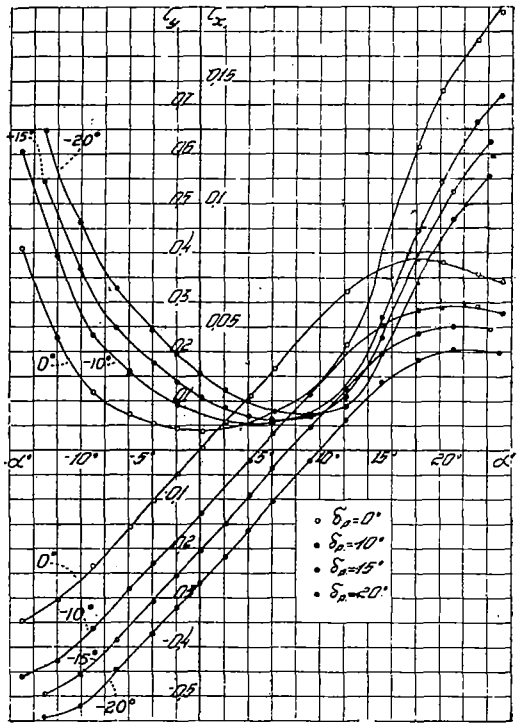

Figure 65.- Tail surface No. 3a.

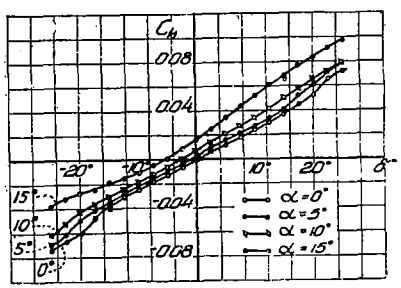

Figure 66.- Tail surface No. 3a.

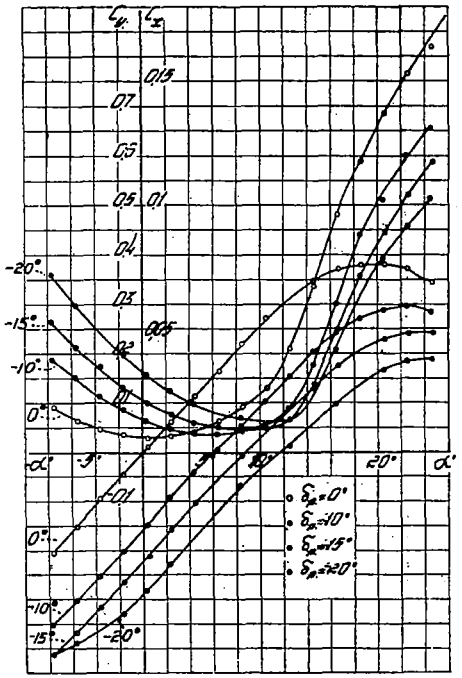

Figure 67.- Tail surface No. 4.

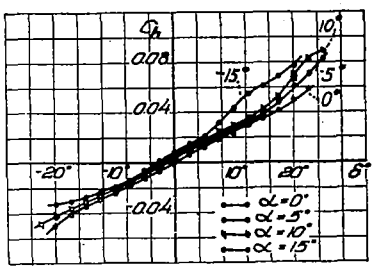

Figure 68.- Tail surface No. 4.

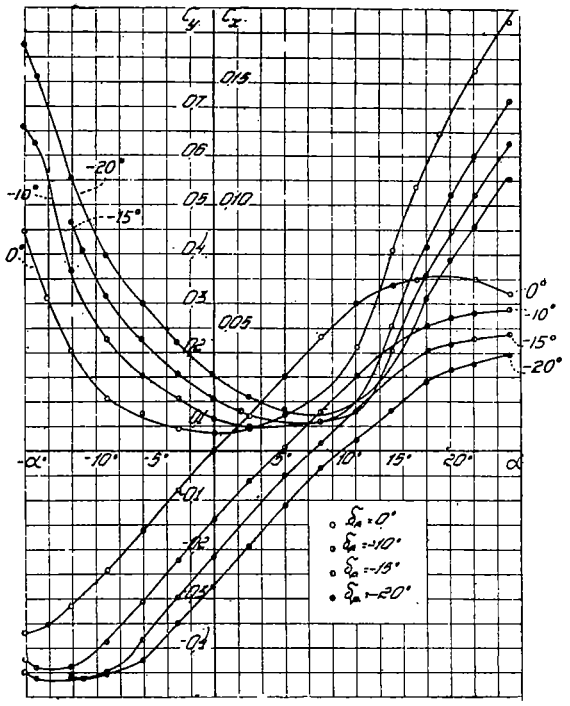

Figure 69.- Tail surface No. 4a.

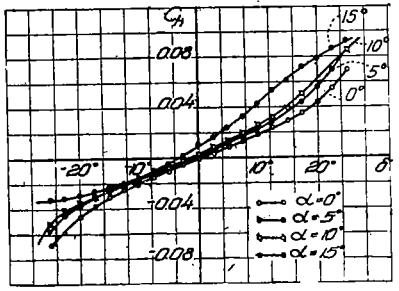

Figure 70.- Tail surface No. 4a.

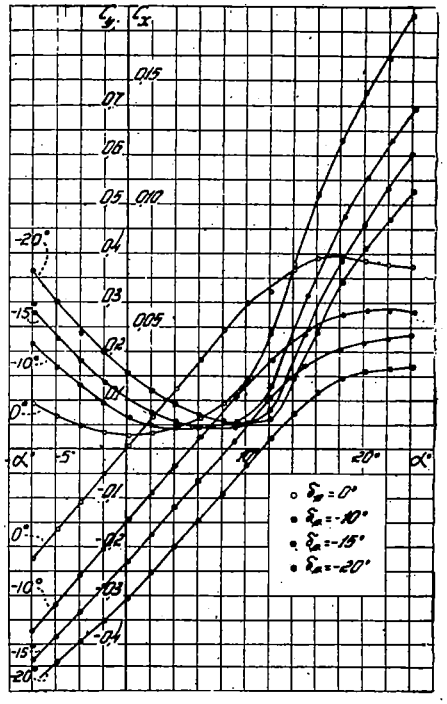

Figure 71.- Tail surface No. 5.

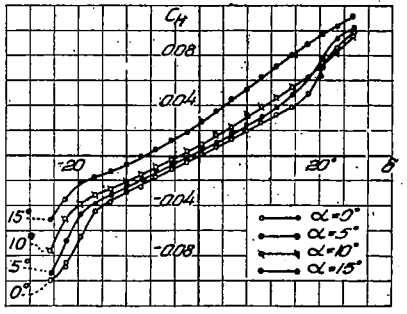

Figure 72.- Tail surface No. 5.

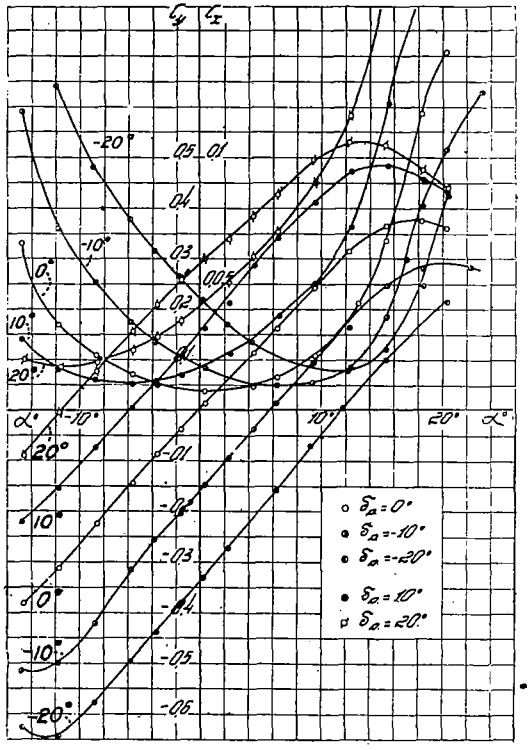

Figure 73.- Tail surface No. 6.

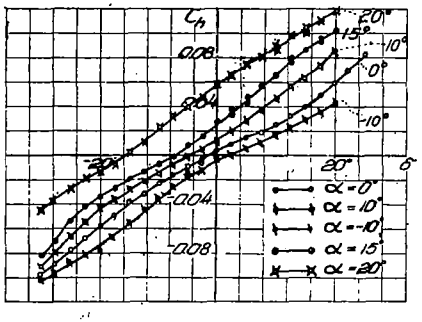

Figure 74.- Tail surface No. 6.

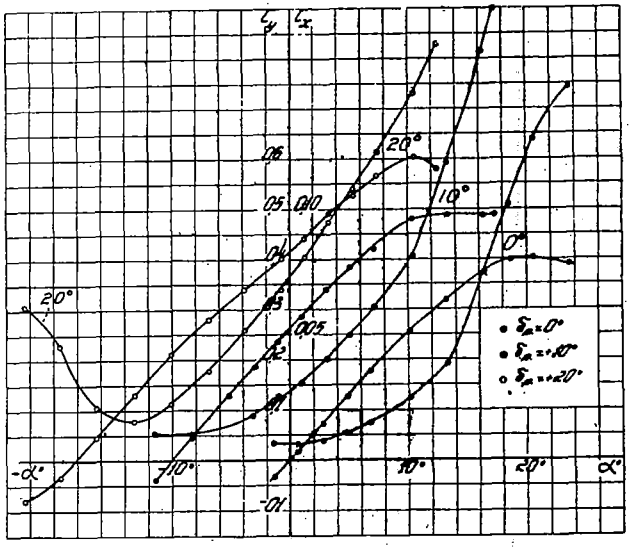

Figure 75.- Tail surface No. 7.

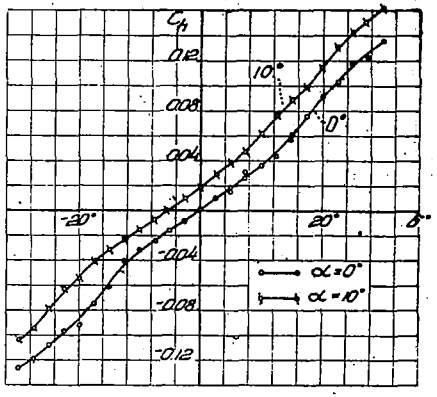

Figure 76.- Tail surface No. 7.

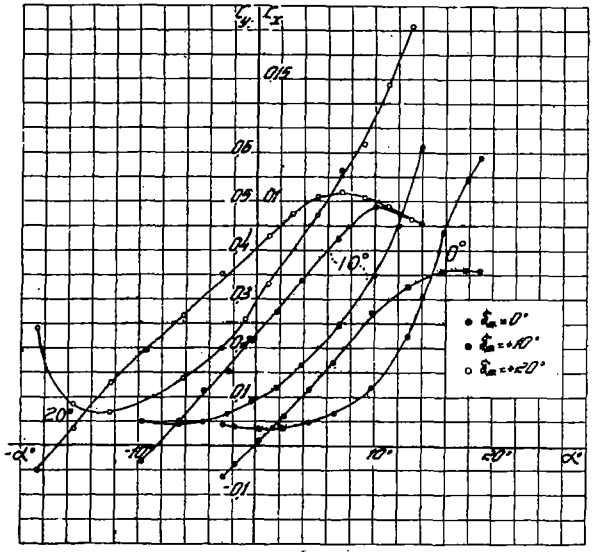

Figure 77.- Tail surface No. 7a.

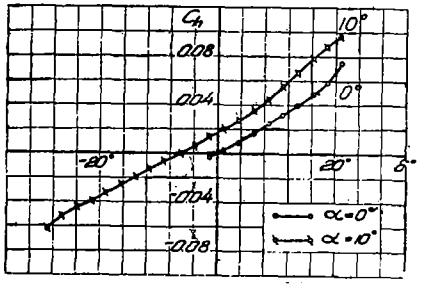

Figure 78.- Tail surface No. 7a.

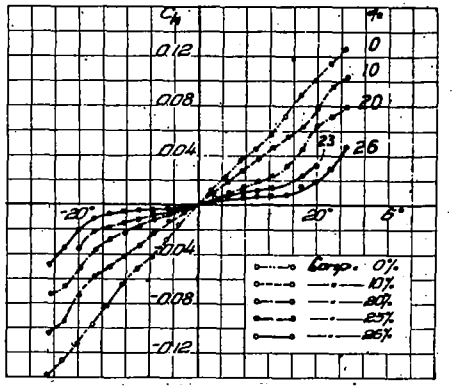

Figure 79.- Tail surface No. 9.

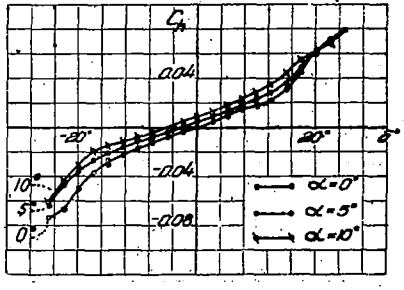

Figure 80.- Tail surface No. 9.

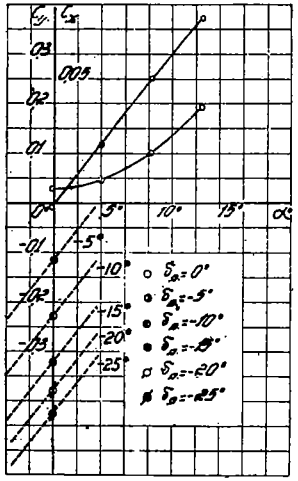

Figure 81.- Tail surface No. 11.

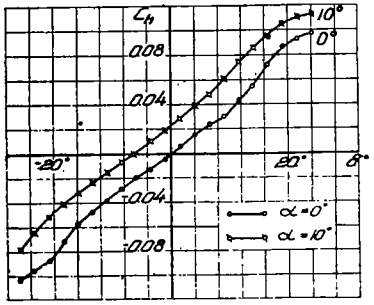

Figure 82.- Tail surface No. 11.

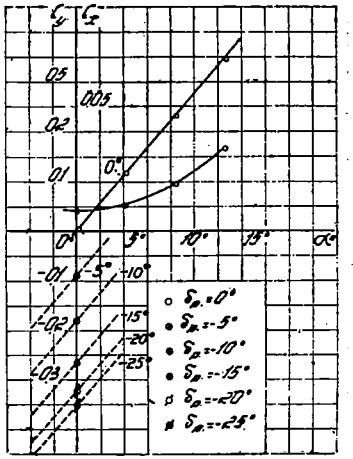

Figure 83.- Tail surface No. 11a.

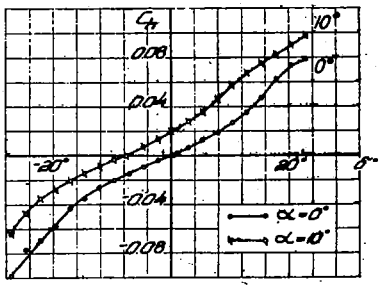

Figure 84.- Tail surface No. 11a.

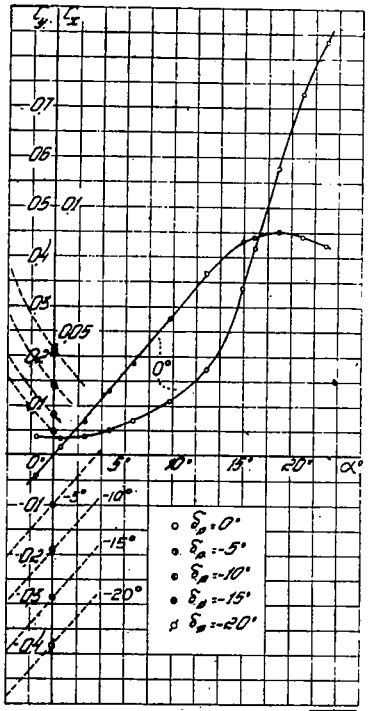

Figure 85.- Tail surface No. 12.

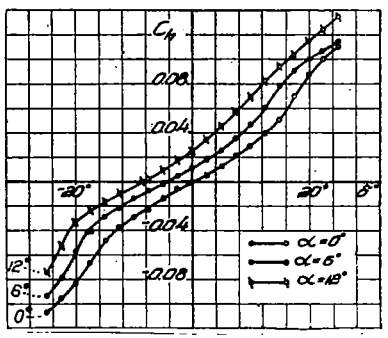

Figure 86.- Tail surface No. 12.

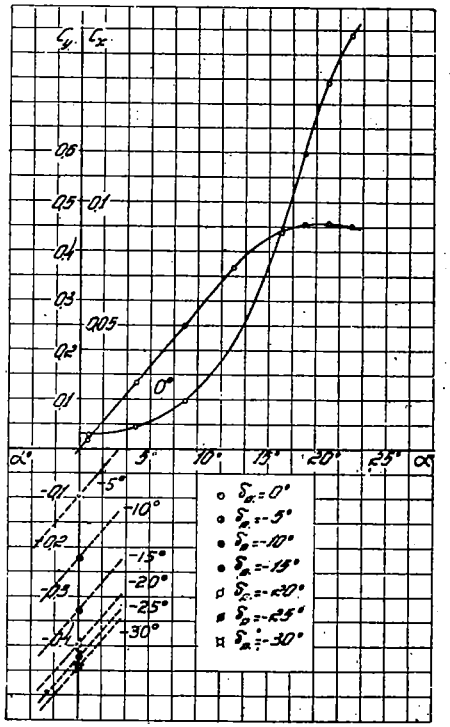

Figure 87.- Tail surface No. 13

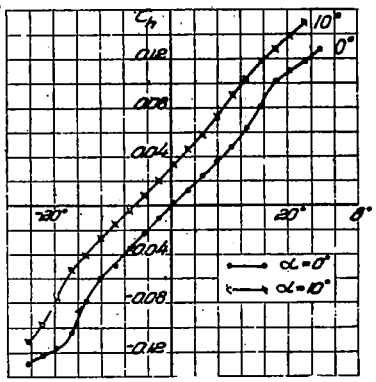

Figure 88.- Tail surface No. 13.

Figs. 85,86,87,88

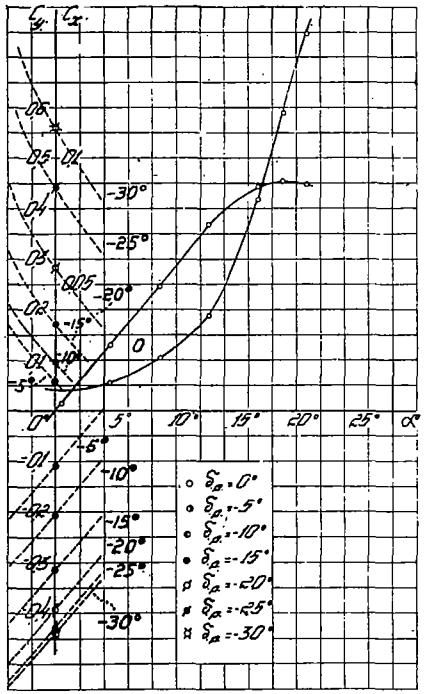

Figure 89.- Tail surface No. 13a.

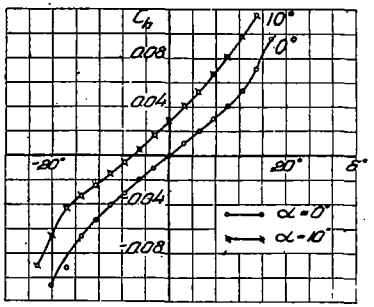

Figure 90.- Tail surface No. 13a.

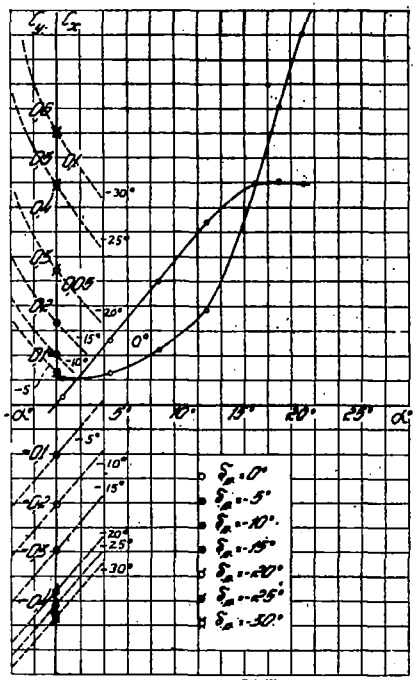

Figure 91.- Tail surface No. 13b.

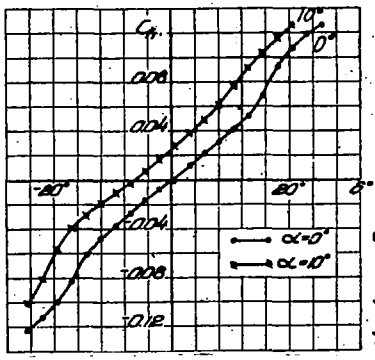

Figure 92.- Tail surface No. 13b.

Figs. 89, 90, 91, 92

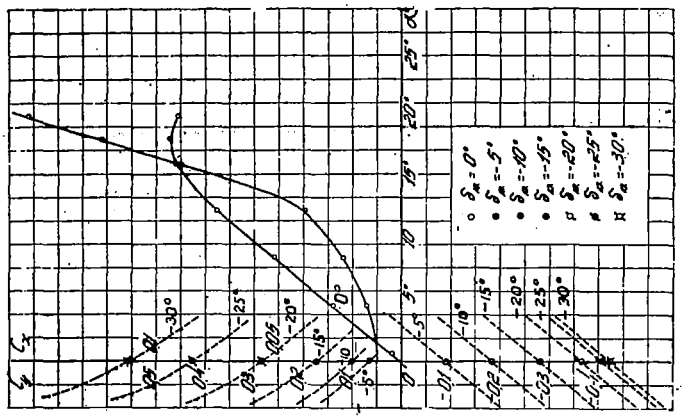

Figure 93.- Tail surface No. 13c.

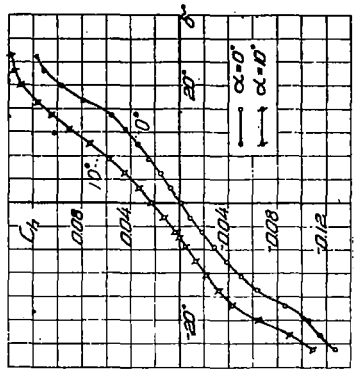

Figure 94.- Tail surface No. 13c.

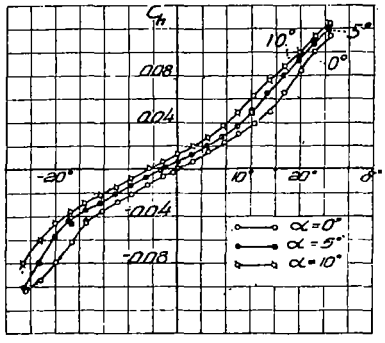

Figure 96.- Tail surface No. 14.

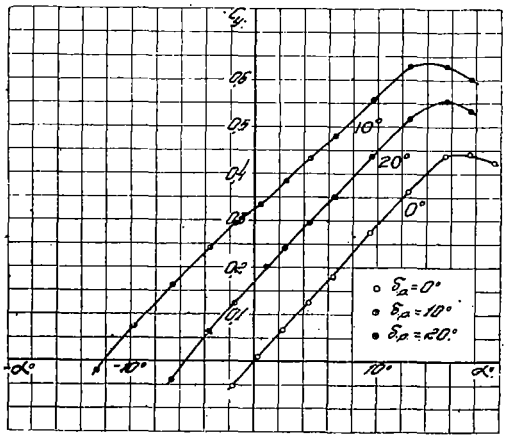

Figure 95.- Tail surface No. 14.

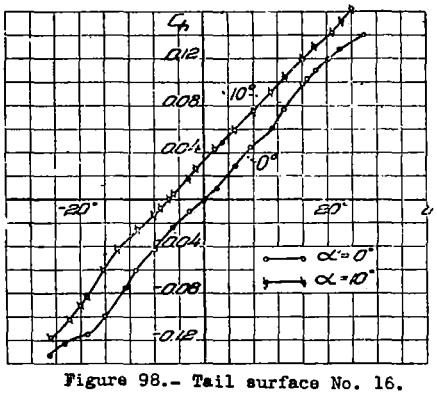

Figure 98.- Tail surface No. 16.

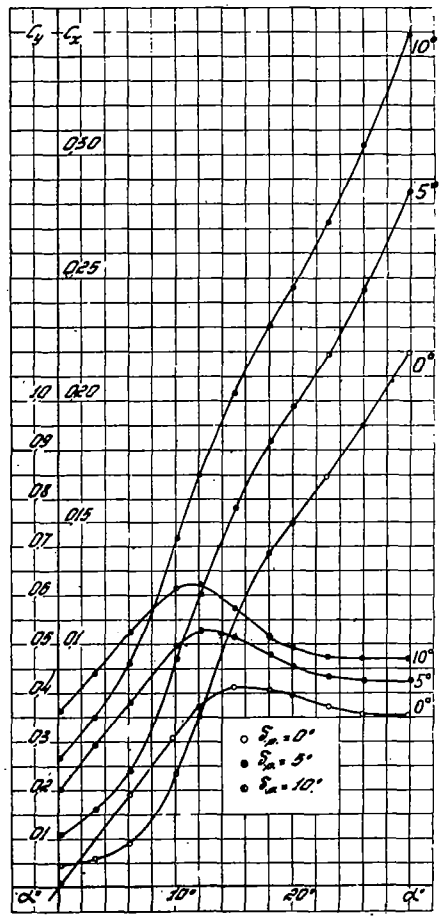

Figure 97.- Tail surface No. 16.

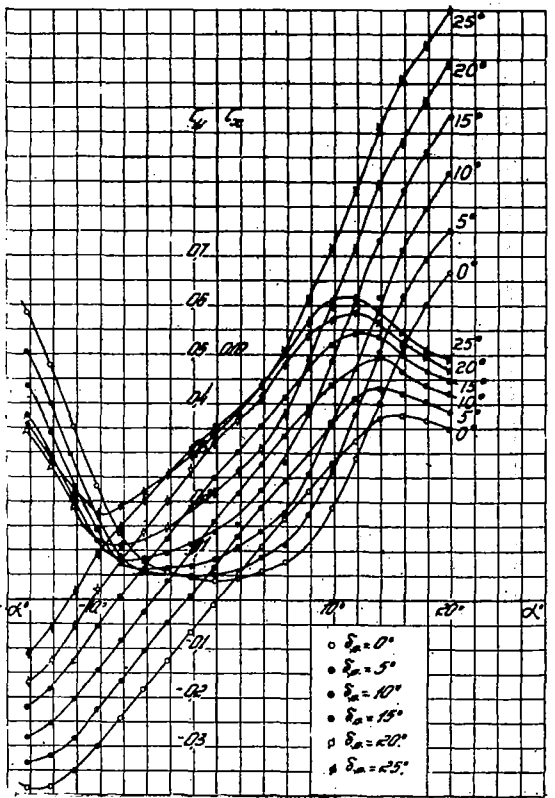

Figure 99.- Tail surface No. 16-1.

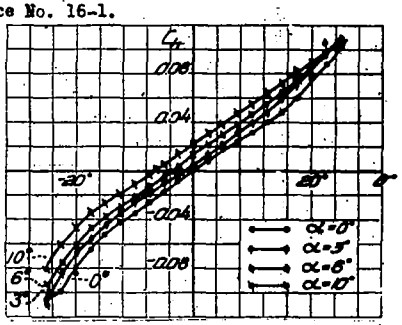

Figure 100.- Tail surface No. 16-1.

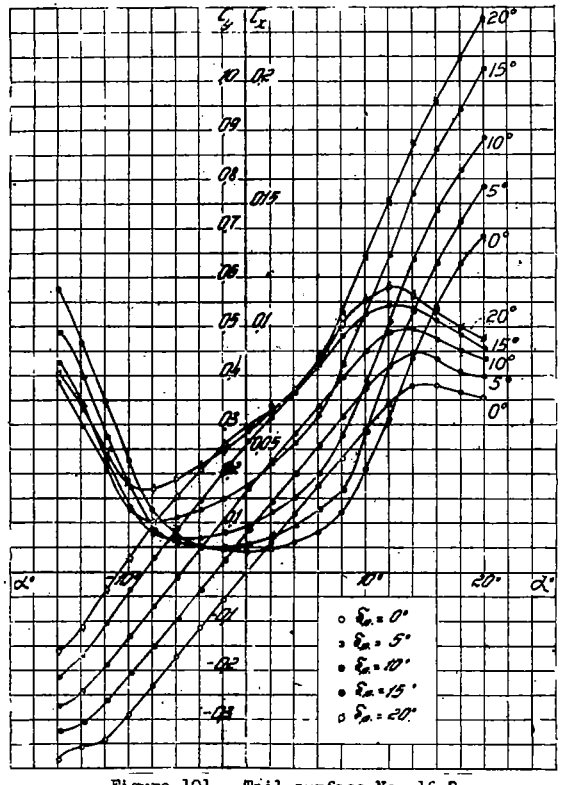

Figure 101.- Tail surface No. 16-2.

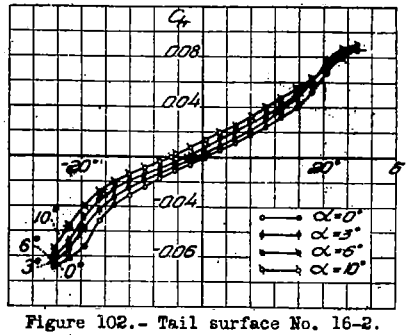

Figure 102.- Tail surface No. 16-2.

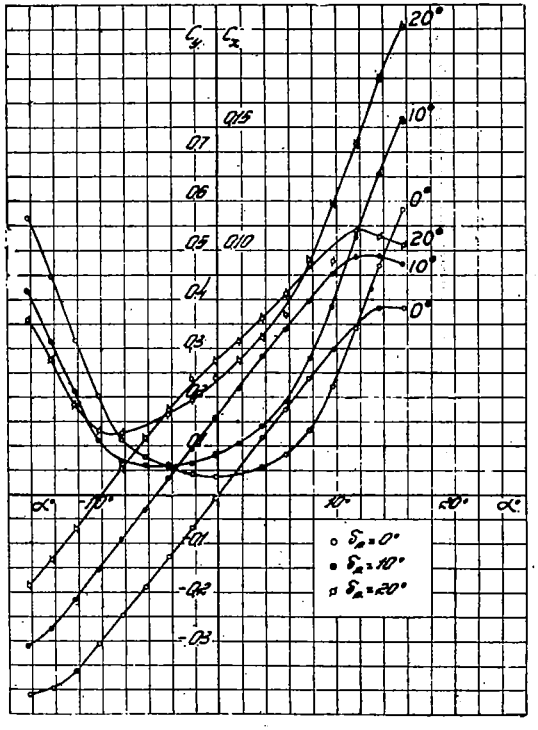

Figure 103.- Tail surface No. 16-3.

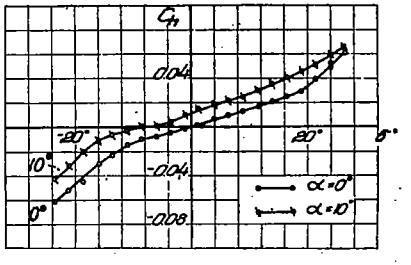

Figure 104.- Tail surface No. 16-3.